농학박사학위논문

Fusarium graminearum 의 열충격반응 관련 유전자 기능연구

Characterization of genes related to heat shock response in *Fusarium graminearum*

2016 년 8 월

서울대학교 대학원

농생명공학부 식물미생물전공

Duc Cuong Bui

Characterization of genes related to heat shock response in *Fusarium graminearum*

A dissertation submitted in partial
fulfillment of the requirement for
the degree of

DOCTOR OF PHILOSOPHY

to the Faculty of
Department of Agricultural Biotechnology

at

SEOUL NATIONAL UNIVERSITY

By

Duc Cuong Bui

August 2016

농학박사학위논문

Fusarium graminearum 의 열충격반응 관련 유전자 기능연구

지도교수 이인원

이 논문을 농학박사학위논문으로 제출함
2016년 6월

서울대학교 대학원
농생명공학부 식물미생물전공

Duc Cuong Bui

Duc Cuong Bui 의 박사학위논문을 인준함
2016년 7월

위 원 장 _____

부위원장 _____

위 원 _____

위 원 _____

위 원 _____

A THESIS FOR THE DEGREE OF DOCTOR OF PHILOSOPHY

Characterization of genes related to heat shock response in *Fusarium graminearum*

UNDER THE DIRECTION OF DR. YIN-WON LEE

SUBMITTED TO THE FACULTY OF THE GRADUATE SCHOOL
OF SEOUL NATIONAL UNIVERSITY

BY
DUC CUONG BUI

MAJOR IN PLANT MICROBIOLOGY
DEPARTMENT OF AGRICULTURAL BIOTECHNOLOGY

JULY 2016

APPROVED AS A QUALIFIED THESIS OF DUC CUONG BUI
FOR THE DEGREE OF DOCTOR OF PHILOSOPHY
BY THE COMMITTEE MEMBERS

CHAIRMAN _____

VICE CHAIRMAN _____

MEMBER _____

MEMBER _____

MEMBER _____

Characterization of genes related to heat shock response in *Fusarium graminearum*

Duc Cuong Bui

ABSTRACT

The *Fusarium* head blight primarily caused by ascomycete *Fusarium graminearum* leads to severe yield losses of various cereal crops and contamination of grains with mycotoxins that are harmful to humans and livestock. The heat shock response involves the induction of a defined set of heat shock proteins which promote the folding of client proteins or target aggregated proteins for degradation, therefore affecting the diverse cellular processes in eukaryotes. In this study, genome-wide transcriptome analysis of cellular adaptation to thermal stress was performed in *F. graminearum*. We found that profound alterations in gene expression were required for heat shock response in *F. graminearum*. Heat shock protein 90 (*Fg*Hsp90) played a central role in heat shock response and *Fg*Hsp90 was exclusively localized to nuclei in response to heat stress. Moreover, the comprehensive functional characterization of *Fg*Hsp90 provides clear genetic evidences supporting its crucial roles in vegetative growth, reproduction, and virulence of *F. graminearum*. Next, the *Fg*Not3

subunit of the Ccr4-Not complex, evolutionarily conserved from yeast to human, was investigated in this fungus. *Fg*Not3 had numerous functions in fungal morphogenesis, sporulation, and virulence. We found that *Fg*Not3 functions as a negative regulator of the production of secondary metabolites, including trichothecenes and zearalenone. Numerous defects of *Fgnot2* and *Fgnot4* deletion mutants, other subunit mutants of the Ccr4-Not complex, demonstrated that the Not module of the Ccr4-Not complex is conserved, and each subunit not only primarily functions within the context of a complex, but also might have distinct roles outside of the complex in *F. graminearum*. This is the first study to functionally characterize the Hsp90 and the Ccr4-Not complex in plant pathogenic fungi and provides novel insights into signal transduction pathways in fungal development.

KEY WORDS: *Fusarium graminearum*, *Fusarium* head blight, heat shock protein 90, Ccr4-Not complex, fungal development, conidiation, sporulation, virulence

Student Number: 2013-30788

TABLE OF CONTENTS

page

CHAPTER 2. The *Fg*Not3 subunit of the Ccr4-Not complex regulates vegetative growth, sporulation, and virulence in *Fusarium graminearum*

page

LIST OF TABLES

page

CHAPTER 1

CHAPTER 2

LIST OF FIGURES

CHAPTER 1

page

CHAPTER 2

Page

CHAPTER 1

Heat shock protein 90 is required for sexual and asexual development, virulence, and heat shock response in *Fusarium graminearum*

ABSTRACT

Eukaryotic cells repress global translation and selectively upregulate stress response proteins by altering multiple steps in gene expression. In this study, genome-wide transcriptome analysis of cellular adaptation to thermal stress was performed on the plant pathogenic fungus *Fusarium graminearum*. The results revealed that profound alterations in gene expression were required for heat shock responses in *F. graminearum*. Among these proteins, heat shock protein 90 (*Fg*Hsp90) was revealed to play a central role in heat shock stress responses in this fungus. *FgHSP90* was highly expressed and exclusively localized to nuclei in response to heat stress. Moreover, our comprehensive functional characterization of *Fg*Hsp90 provides clear genetic evidence supporting its crucial roles in the vegetative growth, reproduction, and virulence of *F. graminearum*. In particular, *Fg*Hsp90 performs multiple functions as a transcriptional regulator of conidiation. Our findings provide new insight into the mechanisms underlying adaptation to heat shock and the roles of Hsp90 in fungal development.

INTRODUCTION

Heat stress affects a broad range of cellular processes that result in cell cycle arrest (Rowley et al. 1993), damage to membranes and cytoskeletal structures (Richter et al. 2010), and accumulation of misfolded proteins (Vidair et al. 1996). To overcome these injuries, eukaryotic cells have evolved delicate heat shock response mechanisms that are primarily mediated by heat shock proteins (Hsps). Hsps are a family of proteins that are produced in response to thermal stress and are involved in various molecular functions, including molecular chaperone activity to assist with proper protein folding and disaggregation (Hendrick and Hartl 1993), cell wall remodelling (Imazu and Sakurai 2005), and maintenance of cell structures (Richter et al. 2010). Although the number and nature of genes involved in the heat shock response vary between organisms, heat shock-related chaperones have been found to be rather conserved in eukaryotes (Richter et al. 2010).

The Hsp90 is one of the most ubiquitous chaperones in eukaryotes, and its complex structure, interactions, and dynamic modifications have been comprehensively studied in humans and yeasts (Jackson 2013). Hsp90, which constitutes 1-2% of the total protein in cytosol, is understood to be essential for the viability of *Saccharomyces cerevisiae* (Borkovich et al. 1989), *Neurospora crassa* (Colot et al.

2006), *Aspergillus fumigatus* (Lamoth et al. 2012), and *Drosophila melanogaster* (Cutforth and Rubin 1994). In *S. cerevisiae*, Hsp90 does not participate in the *de novo* folding of most proteins, but Hsp90 is specifically required for the proper folding of a subset of proteins that exhibits greater difficulty in reaching their native conformations (Nathan et al. 1997). Moreover, Hsp90 directly or indirectly controls the function of at least 10% of the entire proteome (Nathan et al. 1997) and physically interacts with calcineurin (Imai and Yahara 2000). Hsp90 is expressed as two isoforms in human cells, a stress-induced isoform (Hsp90α) and a constitutively expressed isoform (Hsp90β), which perform distinct functions (Johnson 2012). Whereas two Hsp90 orthologues (Hsp82 and Hsc82) have been reported in *S. cerevisiae*, only a single gene for Hsp90 has been identified in *Candida albicans* and in *A. fumigatus* (Lamoth et al. 2014b). Experiments inducing heterologous expression of human Hsp90 in *S. cerevisiae* (Picard et al. 1990) and of *C. albicans* Hsp90 in *S. cerevisiae* (Hodgetts et al. 1996) confirmed that Hsp90s perform conserved biochemical functions in eukaryotes.

Genetic repression utilizing conditional gene expression systems have been applied to study the biological roles of *HSP90*s in fungi including *S. cerevisiae*, *C. albicans*, *C. glabrata*, and *A. fumigatus* because of their lethal nature (Cowen and Lindquist 2005; Cowen et al. 2009; Lamoth et al. 2012; Lamoth et al. 2014a). In *C. albicans*,

repressing *HSP90* using a tetracycline-repressible promoter (*tetO*) results in attenuated virulence in mice (Cowen et al. 2009; Shapiro et al. 2009). Similarly, repressing *HSP90* using a thiamine-repressible promoter (*pthiA*) leads to a complete lack of growth *in vitro* and loss of virulence of *A. fumigatus* (Lamoth et al. 2012; Lamoth et al. 2014a). Moreover, repressing *AfHSP90* induces a defect in asexual sporulation, which is associated with downregulation of the conidiation-specific genes *BRLA*, *WETA*, and *ABAA* (Lamoth et al. 2012). One study of *Af*Hsp90 indicated that observations derived from the model yeast *S. cerevisiae* cannot all be extrapolated to all other fungi. Moreover, little is known about the mechanistic roles of Hsp90 in filamentous fungi, and no Hsp90 orthologue has been functionally characterized in plant pathogenic fungi to date.

The ascomycete fungus *Fusarium graminearum* causes devastating *Fusarium* head blight in major cereal crops worldwide, leading to not only yield and quality losses but also contamination with harmful mycotoxins (Desjardins 2006). *F. graminearum* produces sexual spores (ascospores) within perithecia and asexual spores (conidia) on or within plant residues, including small grain stems and roots as well as maize stalks and ear pieces (Kazan et al. 2012). These spores are resistant to environmental stress conditions and are well suited for dispersal; thus, *F. graminearum* spores act as primary and secondary inocula (Trail et al. 2005). Therefore, sexual and asexual

reproduction by *F. graminearum* are important processes in the development of *Fusarium* head blight, and various genes and genetic pathways have been found to regulate these sporulation processes (Wong et al. 2011; Kazan et al. 2012).

The aim of this study was to further understand the heat shock response in the plant pathogenic fungus *F. graminearum*. As a first step, the RNA-seq-based transcriptome was analyzed under optimal and elevated temperature conditions to identify genome-wide heat shock responses in this fungus. We found that the Hsp90 orthologue of *F. graminearum* plays the most active role in its response to thermal stress. Moreover, the important roles of Hsp90 in the life cycle of *F. graminearum* were investigated using various molecular genetic tools. Consequently, we comprehensively investigated not only the response of plant pathogenic fungi to heat stress but also the specific role of *Fg*Hsp90 in fungal development.

MATERIALS AND METHODS

I. Fungal strains and media

The *F. graminearum* wild-type strain Z-3639 (Bowden and Leslie 1999) and the mutants used in this study are listed in Table 1. Standard laboratory methods and culture media for *Fusarium* species were used (Leslie et al. 2006). For fungal sporulation, conidia of all strains were induced on yeast malt agar (YMA) (Harris 2005) or in carboxymethyl cellulose (CMC) medium (Cappellini and Peterson 1965). The growing temperature of fungal strains was set at 25 ^{o}C unless otherwise specified. The wild-type and transgenic strains were stored as mycelia and conidia in 30% glycerol at -80 °C.

II. Nucleic acid manipulation, primers, and PCR conditions

The genomic DNA was extracted following the standard protocol (Leslie et al. 2006). Restriction endonuclease digestion, agarose gel electrophoresis, gel blotting, and DNA blot hybridization were performed in accordance with standard techniques (Sambrook and Russell 2001). The PCR primers (Table 2) used in this study were synthesized by an oligonucleotide synthesis facility (Bionics, Seoul, Korea).

Table 1. *F. graminearum* strains used in this study.

Strain	Genotype	Reference, source, or parent strains
Z-3639	*Fusarium graminearum* wild-type	(Bowden and Leslie 1999)
hH1-GFP	*hH1::hH1-GFP-HYG*	(Hong et al. 2010)
P_{zear}-*GzmetE*	*GzMETE::HYG-*P_{zear}*-GzmetE*	(Lee et al. 2010)
mat1g	Δ*mat1-1::GEN hH1::hH1-GFP-HYG*	(Hong et al. 2010)
mat1r	Δ*mat1-1::GEN hH1::hH1-RFP-HYG*	(Son et al. 2011a)
HK12	*GFP-HYG* (GFP constitutive expresser)	(Son et al. 2011b)
Δ*mat1*	Δ*mat1-1::GEN*	(Lee et al. 2003)
Δ*mat2*	Δ*mat1-2::GFP-HYG*	(Lee et al. 2003)
KM19	Δ*mat1-1-1::GEN GFP-HYG*	(Min et al. 2012)
HK226	*FgHSP90::HYG-*P_{zear}*-FgHSP90*	This study
HK227	*FgHSP90::FgHSP90-GFP-HYG*	This study
HK301	*FgHSP90::HYG-*P_{zear}*-FgHSP90 hH1::hH1-GFP-HYG*	mat1g×HK226
HK302	*FgHSP90::HYG-*P_{zear}*-FgHSP90 GFP-HYG*	KM19×HK226
HK303	*FgHSP90::FgHSP90-GFP-HYG hH1::hH1-RFP-HYG*	mat1r × HK227
HK167	Δ*mat1-2::GFP-HYG* Δ*abaA::GEN*	This study
AbaAc	Δ*abaA::ABAA-GFP-HYG*	(Son et al. 2013)
HK304	Δ*mat1-1::GEN* Δ*abaA::ABAA-GFP-HYG*	Δ*mat1*× AbaAc
HK305	*FgHSP90::HYG-*P_{zear}*-FgHSP90* Δ*abaA::GEN*	HK167 × HK226
HK306	*FgHSP90::HYG-*P_{zear}*-FgHSP90* Δ*abaA::ABAA-GFP-HYG*	HK304 × HK226

Table 2. Primers used in this study.

Primer	Sequence (5'→3')	Description
FgHSP90-5F pzear	CCAAGTCAATAACTGCGTCCTGTTC	Forward and reverse primers for amplification of 5′-flanking region of *FgHSP90* with tail for the hygromycin resistance gene cassette fusion
FgHSP90-5R pzear	tccactagctccagccaagccAGCCCACCTAGCGCTGCCTA	
FgHSP90-3F pzear	gagagaacgaaagtaaccatgCTCTCACGCTTTTTGCACATTCTCT	Forward and reverse primers for amplification of 3′-flanking region of *FgHSP90* with tail for the geneticin resistance gene cassette fusion
FgHSP90-3R pzear	GCGTACTCGTCAATGGGGTCAA	
FgHSP90-5N pzear	TCATTGTGGTGGGAGAGGTGGTAG	Forward and reverse nest primers for third fusion PCR for amplification of the *FgHSP90* repression construct
FgHSP90-3N pzear	TCTTGGAGAAGGCGCTGTAGAACTT	
HYG-F1	GGCTTGGCTGGAGCTAGTGGAGG	Forward and reverse primers for amplification of P_{zear} with hygromycin resistance gene cassette from the P_{zear}-*GzmetE* strain
zear-r2	CATGGTTACTTTCGTTCTCTCTGGTC	
pIGPAPA-sGFP	GTGAGCAAGGGCGAGGAGCTG	Forward primer for amplification of the GFP-HYG construct from pIGPAPA vector
FgHSP90-5F GFP	CCAGCGCTGGTGGTACTTTCTCC	Forward and reverse primers for amplification of 5′-flanking region for Gfp tagging *FgHSP90* with tail for the
FgHSP90-5R GFP	gaacagctcctcgcccttgctcacGTCGACCTCCTCCATGGC	

		hygromycin resistance gene cassette fusion
FgHSP90-3F GFP	cctccactagctccagccaagccCCTTTTTCGGATGGGGTGTAACTC	Forward and reverse primers for amplification of 3′-flanking region for Gfp tagging *FgHSP90* with tail for the hygromycin resistance gene cassette fusion
FgHSP90-3R GFP	TGCACGCTAGTCCAAGAATACGG	
FgHSP90-gfpF	GTACCTCCATCATCCTCCACCTCAA	Forward and reverse nest primers for third fusion PCR for amplification of Gfp tagging *FgHSP90* construct
FgHSP90-gfpR	CCTGATCCTGAGGGGTCTGACAG	
HSP90-rt-F	AGTTCCGTGCCATCCTCTTCGT	For realtime-PCR of *HSP90*
HSP90-rt-R	GCGGACGTAGAGCTTGATGTTGTT	
STUA-rt-F	CAGAACGGAAATGATGGTGGACTC	For realtime-PCR of *STUA*
STUA-rt-R	ATTGGAAAGAGGCTGGTGAAGGT	
HTF1-rt-F	GGAAGAAGAGCTGAGGTGGGACAT	For realtime-PCR of *HTF1*
HTF1-rt-R	TGGAAGTTGGGGGAGCGGT	
REN1-rt-F	ACGACAGACTTGAATCGCCTGACA	For realtime-PCR of *REN1*
REN1-rt-R	TATCGTGCCACATCGTATCCAGCA	
ABAA-rt-F	ACTCAGGAAGCTTTGACCACGGC	For realtime-PCR of *ABAA*
ABAA-rt-R	GGGCTCTGGTAGGGGTTGACAGTA	
WETA-rt-F	GTTCCAGGTACTCCCACTGCCAT	For realtime-PCR of *WETA*
WETA-rt-	ACGTTCTCGTCGCGCTTTGG	

R	T	
UBH-rt-F	GTTCTCGAGGCCAGCAAAAAGTCA	For realtime-PCR of *UBH*
UBH-rt-R	CGAATCGCCGTTAGGGGTGTCTG	
16768-rt-F	CACCGCTGGCTCTGACATTGA	For realtime-PCR of FGSG_16768
16768-rt-R	GCAGCGAGCTAGGACGAGTGAAT	
10816-rt-F	CCTTCCAACCCAGCTATGACACC	For realtime-PCR of FGSG_10816
10816-rt-R	CTGCACCATCCTGAGAGAAGCG	
08768-rt-F	TCGTGGCGGTATGCAAATCTTC	For realtime-PCR of FGSG_08768
08768-rt-R	AAAATTTGCATACCACCACGAAGG	
03247-rt-F	CACATACCCATCCGTCAGCAAACT	For realtime-PCR of FGSG_03247
03247-rt-R	GATGCGGAACCAGTCAAGAATGTC	
00766-rt-F	AGAAGGCCATGGATGCTGAAGTT	For realtime-PCR of FGSG_00766
00766-rt-R	GAAGATCTCGGAGGCGTTGGA	
02316-rt-F	CATCTTCGCCCCCGTTCTGA	For realtime-PCR of FGSG_02316
02316-rt-R	GTGCGAGCATCTGTTTTGAGGAA	

III. Genetic modifications

To replace the *FgHSP90* promoter with P_{zear}, the hygromycin resistance gene cassette (*HYG*)-P_{zear} was amplified from the P_{zear}-*GzmetE* strain (Lee et al. 2010) using the HYG-F1 and zear-r2 primers, and the 5′ and 3′ flanking regions of the *FgHSP90* gene were amplified from Z-3639 using the primers FgHSP90-5F pzear/FgHSP90-5R pzear and FgHSP90-3F pzear/FgHSP90-3R pzear, respectively. The resulting three fragments were fused according to the double-joint (DJ) PCR method (Yu et al. 2004), and the final construct was amplified using the primers FgHSP90-5N pzear/FgHSP90-3N pzear. To induce P_{zear} replacement, 30 μM β-est was added to the medium during the regeneration, overlay, and mutant selection processes (Lee et al. 2010).

To generate *GFP*-tagged *Fg*Hsp90 strains, the *GFP-HYG* fragment was amplified from the pIGPAPA plasmid (Horwitz et al. 1999) using the primers pIGPAPA-sGFP/HYG-F1. The 5′ and 3′ flanking regions of the *FgHSP90* gene were amplified from Z-3639 using the primers FgHSP90-5F GFP/FgHSP90-5R GFP and FgHSP90-3F GFP/FgHSP90-3R GFP, respectively. After fusion PCR, the resulting PCR product was used as a template together with the primers FgHSP90-gfpF and FgHSP90-gfpR to produce the final construct. Subsequently, the final PCR products were transformed into the Z-3639 strain.

IV. Conidial production

After each strain was incubated in 50 ml of complete medium (CM) for 72 h at 25 °C on a rotary shaker (150 rpm), mycelia of each strain were harvested and washed twice with distilled water. To induce conidiation, 72 h-old mycelia were spread on YMA and incubated for 48 h at 25 °C under near-UV light (wavelength: 365 nm, HKiv Import & Export Co., Ltd., Xiamen, China). Conidia were collected using distilled water, filtered through cheesecloth, washed, and resuspended in distilled water. After inoculating a 1-ml conidial suspension (1×10^6 conidia/ml) of each strain in 50 ml of CMC and incubating this culture for 5 days at 25 °C on a rotary shaker (150 rpm), the number of conidia produced was counted using a haemocytometer (Superior, Marienfeld, Germany) to measure conidial production.

V. Sexual development and virulence tests

Mycelia grown on carrot agar for 5 days were mock-fertilized with sterile 2.5% Tween 60 solution to induce sexual reproduction as previously described (Leslie et al. 2006). After sexual induction, the fertilized cultures were incubated for 7 days under near-UV light (HKiv Import & Export Co., Ltd.) at 25 °C.

A virulence test of the fungal strains was performed using the wheat cultivar Eunpamil as previously described (Son et al. 2011a).

Briefly, 10 µl of a conidial suspension (1×10^5 conidia/ml) obtained from each strain was point-inoculated onto a spikelet of the wheat head at early anthesis. Inoculated plants were incubated in a humidified chamber for 3 days and subsequently transferred to a greenhouse. After 21 days, the number of spikelets showing disease symptoms was counted.

VI. Microscopic observation

Microscopic observation was performed using a DE/Axio Imager A1 microscope (Carl Zeiss, Oberkochen, Germany) equipped with the filter set 38HE (excitation 470/40; emission 525/50) for Gfp and the filter set 15 (excitation 546/12; emission 590) for Rfp.

Wheat heads inoculated with the Gfp-tagged strains were sampled 6 days after inoculation. Freehand longitudinal sections across the centre of the spikelets were prepared using a clean scalpel (Baldwin et al. 2010). Sectioned wheat heads were observed under reflected light and Gfp-fluorescent light (470-nm excitation and 525-nm emission wavelength filters) using a SteREO Lumar V12 microscope (Carl Zeiss).

VII. qRT-PCR

Mycelia were harvested via filtration through one or two layers of Miracloth, washed with water, frozen in liquid nitrogen, lyophilized, and ground in a mortar and pestle prior to RNA extraction using the Easy-Spin total extraction kit (iNtRON Biotech, Seongnam, Korea). First-strand cDNA was synthesized with the SuperScript III First-Strand Synthesis System (Invitrogen, Carlsbad, CA, USA) using oligo$(dT)_{20}$ according to the manufacturer′s recommendations. qRT-PCR was performed using iQ SYBR Green Master Mix (Bio-Rad, Hercules, CA, USA) and a 7500 real-time PCR system (Applied Biosystems, Foster City, CA, USA). The endogenous housekeeping gene ubiquitin C-terminal hydrolase (*UBH*; FGSG_01231) was used for normalization (Kim and Yun 2011). The PCR assays were repeated three times with two biological replicates. The transcript level relative to that of the housekeeping gene was expressed as $2^{-\Delta\Delta CT}$ (Livak and Schmittgen 2001).

VIII. RNA-seq and bioinformatic analysis

Conidia were inoculated in CM for 12 h at 25 °C and then further incubated at 37 °C for 15 min for heat shock treatment. Total RNA was extracted using the Easy-Spin total extraction kit (iNtRON Biotech) as described above. RNA-seq libraries were created using the

Illumina TruSeq RNA sample preparation kit strictly according to the standard low-throughput protocol. Sequencing was performed using an Illumina HiSeq 2000 instrument and the reagents provided in the Illumina TruSeq paired-end (PE) Cluster kit v3-cBot-HS and the TruSeq SBS kit v3-HS (200 cycles). Each experiment was repeated three times, and mean values were used for bioinformatic analyses.

The data have been deposited in NCBI's Gene Expression Omnibus (Barrett et al. 2013) and are accessible at GEO Series accession number GSE78885 (http://www.ncbi.nlm.nih.gov/geo/query/acc.cgi?acc=GSE78885). The genome-wide transcript levels of genes were quantified as RPKHM (Mortazavi et al. 2008). When the RPKHM value was 0, it was changed to 1 to calculate the fold change of the transcript level.

RESULTS

I. Heat shock causes a profound modification of gene expression in *F. graminearum*

To dissect cellular responses to thermal stress in *F. graminearum*, we compared the transcriptomes of fungal cultures incubated under optimal (25 °C) and high temperature conditions (37 °C) for 15 min. Based on a threshold of reads per kilobase of exon per hundred million mapped reads (RPKHM) values (≥10) under all tested conditions, 9,638 out of 13,820 genes (Wong et al. 2011) were selected for further analyses. Differentially expressed genes (DEGs) were identified as genes displaying a greater than two-fold change in transcript levels. Compared with optimal growth conditions (25 °C), heat shock conditions induced the differential expression of 5,983 genes (1,975 genes were upregulated and 4,008 genes were downregulated). These results emphasise a profound modification of gene expression, such that ~43% of the total genes were differentially expressed in this fungus.

Gene ontology (GO) enrichment analysis was applied to classify the functions of the predicted DEGs, and the GO terms were statistically analyzed using GOstats and subsequently visualized using REVIGO. REVIGO provides a network structure of non-redundant GO terms (Fig. 1a) and produces clustered images (TreeMap) based on

semantic similarity among GO terms (Table 3). The highly expressed genes were assigned to 111 categories; 51 were included in biological process, 48 in molecular function, and 12 in cellular component (Fig. 1a). Accordingly, the most significant GO terms included “lipid storage”, “response to stress”, “nuclear division”, and “carbohydrate derivative catabolism” (biological process); “transporter activity” and “tRNA-intron endonuclease activity” (molecular function); and “nucleus”, “hyphal cell wall”, and “intrinsic component of membrane” (cellular component) (Table 3 and Fig. 1a). Alternatively, downregulated genes were assigned to 209 categories (108 in biological process, 47 in molecular function, and 44 in cellular component). The GO terms corresponding to negatively regulated genes under thermal stress conditions included “amide biosynthetic process”, “cellular metabolic process”, “protein binding”, and “ribosomal subunit” (Table 3).

Pathway analyses were performed using the Kyoto Encyclopedia of Genes and Genomes (KEGG) database. The metabolic pathways showing significant induction by heat stress were “tryptophan metabolism”, “aminobenzoate degradation”, “fatty acid degradation”, “beta-alanine metabolism”, and “caffeine metabolism”; however, “citrate cycle”, “aminoacyl-tRNA biosynthesis”, “histidine metabolism”, “terpenoid backbone biosynthesis”, and “lysine biosynthesis” were repressed by heat stress (Fig. 1b).

We evaluated the transcript levels of genes possibly related to thermal stress responses based on GO terms (GO: 0009266, response to temperature stimulus; GO: 0009408, response to heat; GO: 0034605, cellular response to heat) and found only seven DEGs among 44 genes (Table 4). Notably, a ubiquitous chaperone, heat shock protein 90 (*Fg*Hsp90, FGSG_02014), was revealed to be most highly induced under heat stress conditions. In addition, the co-chaperone with Hsp90 (FGSG_00766, *STI1*) and one ubiquitin gene (FGSG_08768, *UBI4*) were highly expressed under high temperature conditions. The transcript levels were further confirmed using quantitative real-time (qRT)-PCR.

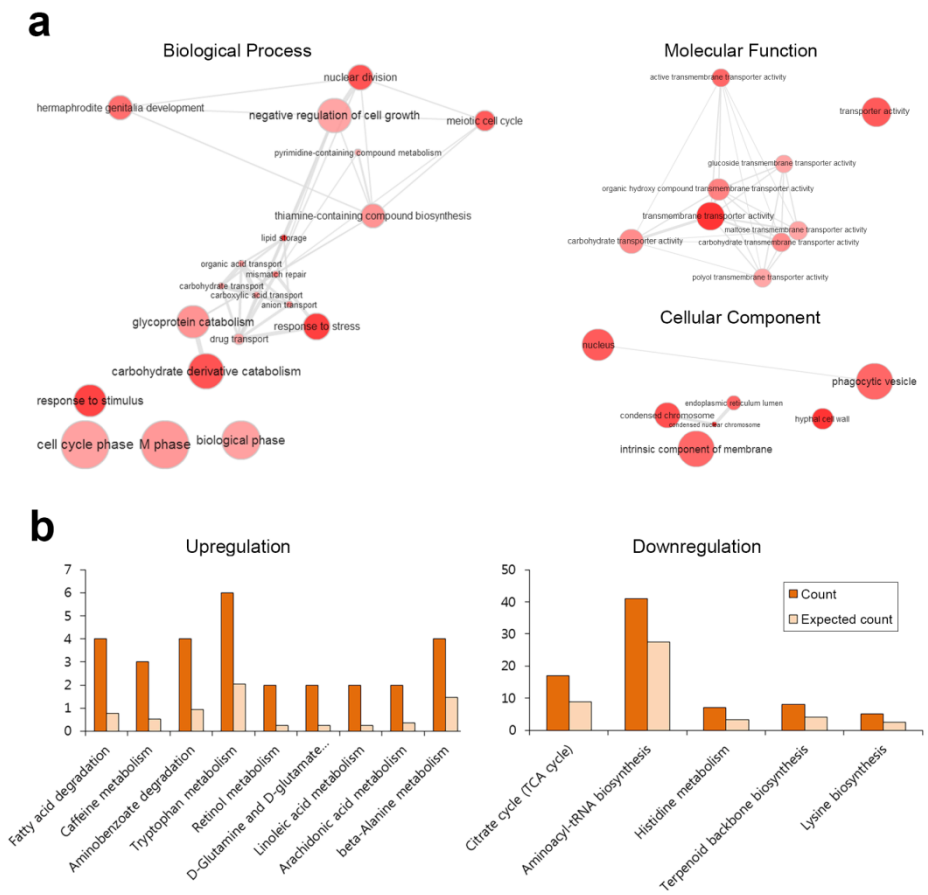

Figure 1. RNA-seq-based transcriptome analysis of the *F. graminearum* wide-type strain under heat shock stress. (**a**) GO enrichment network of the upregulated genes constructed using REVIGO. (**b**) The biological pathways of the up- and downregulated genes based on the KEGG database (http://www.genome.jp/kegg). These GO terms and KEGG pathways were statistically analyzed using GOstats.

Table 3. Gene Ontology (GO) functional enrichment analysis of up- and downregulated genes during heat shock stress in *F. graminearum*. GO terms; %, percentage of DEGs corresponding to a given GO term among all GO terms in that category.

Representative GO term	Description	%
Upregulation		
Biological process		
GO:0019915	lipid storage	24.7
GO:0006950	response to stress	23.6
GO:0000280	nuclear division	10.1
GO:1901136	carbohydrate derivative catabolism	10.9
Molecular function		
GO:0005215	transporter activity	56.9
GO:0000213	tRNA-intron endonuclease activity	27.8
Cellular component		
GO:0005634	nucleus	71.9
GO:0030446	hyphal cell wall	15.4
GO:0031224	intrinsic component of membrane	12.7
Downregulation		
Biological process		
GO:0043604	amide biosynthetic process	56.3
GO:0044237	cellular metabolic process	10.7
GO:0015031	protein transport	8.5
GO:0034622	cellular macromolecular complex assembly	5.7
GO:0044238	primary metabolic process	5.1
Molecular function		
GO:0005488	binding	27.6
GO:0005515	protein binding	27.1
GO:0003743	translation initiation factor activity	10.7
GO:0016757	transferase activity, transferring glycosyl groups	6.4
GO:0003735	structural constituent of ribosome	6.2
Cellular component		
GO:0044391	ribosomal subunit	75.2
GO:0032991	macromolecular complex	10.4

Table 4. Transcript levels of genes involved in responses to temperature. RPKHM, reads per kilobase of exon per hundred million mapped sequence reads (Mortazavi et al. 2008); 25 °C and 37 °C, transcript levels of genes expressed at 25 °C and 37 °C, respectively; qRT-PCR, the fold-change in gene expression at 37 °C relative to that at 25 °C confirmed by qRT-PCR analysis.

Locus	MIPS annotation	GO term	Mean RPKHM		qRT-PCR
			25 ºC	37 ºC	
FGSG_02014	probable heat shock protein 90	GO:0009266, GO:0009408	18,507	885,938	67.5 ± 5.3
FGSG_00766	related to stress-induced protein *STI1*	GO:0009266, GO:0009408	17,184	318,411	38.2 ± 2.0
FGSG_10816	related to aquaporin	GO:0009266	12	196	54.3 ± 8.4
FGSG_03247	probable *GUT1* - glycerol kinase	GO:0009266	40	523	42.7 ± 2.5
FGSG_08768	probable *UBI4* - ubiquitin	GO:0009266, GO:0009408, GO:0034605	49,752	514,937	23.9 ± 0.8
FGSG_16768	related to Krüppel protein	GO:0009266	912	6454	23.5 ± 4.3
FGSG_02316	related to multidrug resistance protein	GO:0009266, GO:0009408	451	1078	5.9 ± 0.5

II. Transcription of *FgHSP90* is induced in response to heat stress and during sexual and asexual development

qRT-PCR confirmed that the transcript level of *FgHSP90* was dramatically increased in response to elevated temperature (Fig. 2a). Further, the transcript profiles of *FgHSP90* were examined throughout vegetative growth as well as in the stages of asexual and sexual development to elucidate the roles of *FgHSP90* in the life cycle of *F. graminearum*. Although the transcript levels of *FgHSP90* were constitutively maintained during the vegetative growth stages, the *FgHSP90* transcript levels were significantly increased 3 days after sexual induction, followed by a decrease 3 days later (Fig. 2a). Notably, the *FgHSP90* transcript level peaked 4 h after conidial induction and gradually decreased thereafter (Fig. 2a). Taken together, these results indicate that *Fg*Hsp90 is closely involved in sexual and asexual developmental processes as well as heat shock responses in *F. graminearum*.

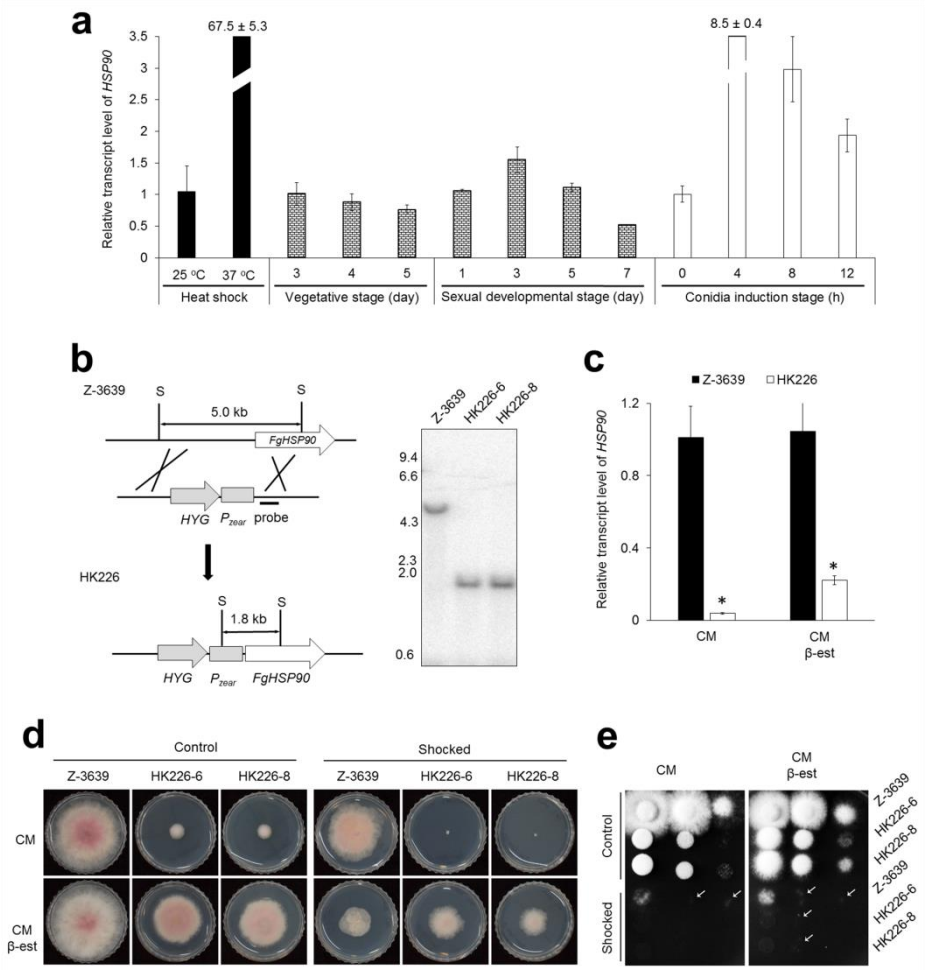

Figure 2. Characterization of the mutant containing the *FgHSP90* gene under the control of a ZEA-inducible promoter (P_{zear}). (**a**) Expression profile of the *FgHSP90* gene in the *F. graminearum* wild-type strain Z-3639 under heat shock conditions and during development. Transcript levels were analyzed via qRT-PCR after heat shock treatment at 37 °C for 15 min, during the vegetative and sexual induction stages on carrot agar, and during conidia induction on YMA medium. During the vegetative and sexual induction stages, the transcript level of *FgHSP90* at the 3-day vegetative stage was

arbitrarily set to 1, and this value was used for comparison to other periods. During the conidial induction stage, the expression of *FgHSP90* at 0 h was arbitrarily set to 1, and this value was used for comparison to other periods. (**b**) An overview of the strategy for promoter replacement. Southern blot hybridization assay confirmed that the Z-3639 strain (lane 1) migrated as a 5.0 kb fragment, but the positively mutated strains HK226-6 and HK226-8 (lanes 2 and 3, respectively) migrated as 1.8-kb bands. (**c**) Confirmation of chemical complementation. The transcript level of *FgHSP90* in the Z-3639 and HK226 strains was analyzed by qRT-PCR. The relative transcript levels in the wild-type strain were arbitrarily set to 1. (**d**) Mycelial growth of *F. graminearum* strains under heat shock conditions. Both wild-type HK226 strains were incubation for 30 min at 48 °C for heat shock stress in the absence and presence of β-est. The images were captured at 3 days after inoculation. (**e**) Serial dilutions of all strains were point-inoculated onto CM with and without β-est after 30 min heat shock treatment at 48 ^{o}C. Arrowheads indicate mycelial growth.

III. Molecular characterization of *Fg*Hsp90

Hsp90 proteins in eukaryotes range in size from 588 to 854 amino acids (Johnson 2012). BLASTp searches for both Hsp82 and Hsc82 from *S. cerevisiae* in the *F. graminearum* genome (Wong et al. 2011) identified the FGSG_02014 locus encoding 700 amino acids (73% and 74% identity with *Sc*Hsp82 and *Sc*Hsc82, respectively). The encoded protein harboured two important domains (IPR004358 and IPR001404) similar to those in both *Sc*Hsp82 and *Sc*Hsc82 (Fig. 3a). Our result was in agreement with the previously characterized *A. fumigatus* orthologue *Af*Hsp90, which consists of 706 amino acids and displays approximately 75% identity to the yeast Hsp90 orthologues (Lamoth et al. 2014b). Whereas human and *S. cerevisiae* carry two Hsp90 homologues, a single Hsp90 isoform is carried by other fungi including *C. albicans*, *Podospora anserina*, and *A. fumigatus* (Loubradou et al. 1997; Johnson 2012; Lamoth et al. 2014b). Based on these results, we designated the protein encoded by FGSG_02014 and referred to this protein as *Fg*Hsp90, a unique orthologue of Hsp90 in *F. graminearum*.

*Fg*Hsp90 contains a nuclear localization sequence (NLS; 246-KPKTKK-251) at its N-terminus (Fig. 3a). Similar to other Hsp90 isoforms in eukaryotes, two evolutionary conserved motifs, NKEIFL and MEEVD, were present in *Fg*Hsp90 (Fig. 3b). The MEEVD motif is

known to interact with tetratricopeptide repeat domains of the co-chaperone Hsp90-Hsp70 organizing protein (Hop, also known as p60 or Sti1) in humans and yeast and is therefore important for the transfer of client proteins from Hsp70 to Hsp90 (Lee et al. 2012). Phylogenetic analyses of Hsp90 orthologues showed that Hsp90s of filamentous fungi were clustered into a separate group relative to Hsp90 from other organisms (Fig. 3c).

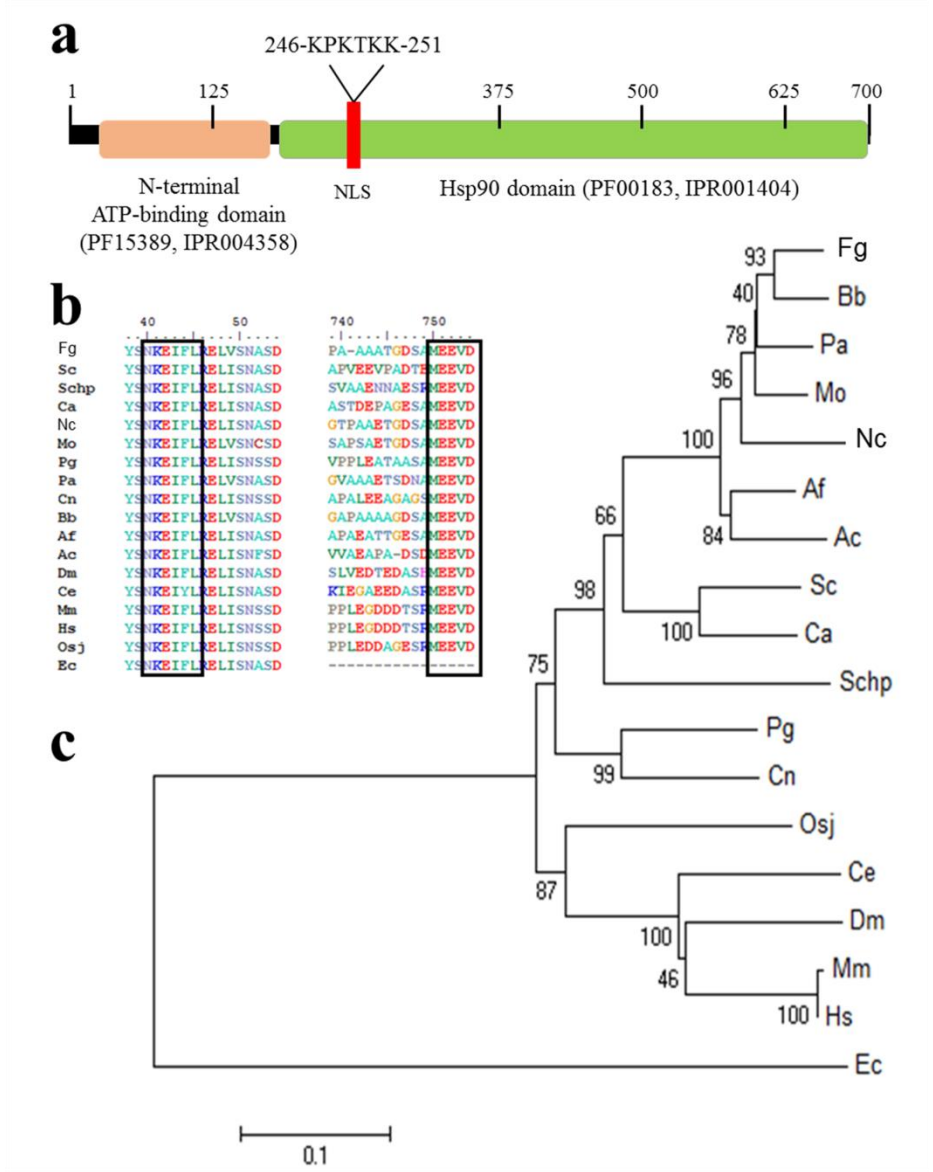

Figure 3. Molecular characterization of *Fg*Hsp90. (**a**) Schematic presentation of the conserved protein domains of *Fg*Hsp90 in *F. graminearum* by InterPro database (http://www.ebi.ac.uk/interpro/) and the HMMPham database (http://pfam.sanger.ac.uk/). NLS, nuclear localization signal predicted by NLStradamus (Ba et al. 2009). (**b**) The eukaryotic evolutionary Hsp90 protein motifs, NKEIFL and MEEVD, are also conserved in *F. graminearum* based on the alignment of

*Fg*Hsp90 amino acid sequence with other representative species, including bacteria, yeasts, filamentous fungi, plant, and animals. Fg, *Fusarium graminearum*; Bb, *Beauveria basiana*; Pa, *Podospora anserina*; Mo, *Magnaporthe oryzae*; Nc, *Neurospora crassa*; Af, *Aspergillus fumigatus*; Ac, *Ajellomyces capsulatus*; Sc, *Saccharomyces cerevisiae*; Ca, *Candida albicans*; Schp, *Schizosaccharomyces pombe*; Pg, *Puccinia graminis*; Cn, *Cryptococcus neoformans*; Osj, *Oryza sativa japonica*; Ce, *Caenorhabditis elegans*; Dm, *Drosophila melanogaster*; Mm, *Mus musculus*; Hs, *Homo sapiens*; Ec, *Escherichia coli*. (**c**) Phylogenetic tree of homologs of the Hsp90 from representative species constructed using amino acid sequences comparison.

IV. *FgHSP90* is an essential gene in *F. graminearum*

As a first step towards investigating the genetic function of *FgHSP90* in *F. graminearum*, we attempted to delete this gene using the homologous recombination method (Yu et al. 2004). Because more than three repeated attempts to delete *FgHSP90* had failed, we concluded that *FgHSP90* is an essential gene in *F. graminearum*, as in yeasts and other filamentous fungi (Borkovich et al. 1989; Colot et al. 2006; Lamoth et al. 2012; Lamoth et al. 2014a). Next, we utilized a conditional gene expression system to repress *FgHSP90*. The zearalenone (ZEA)-inducible promoter (P_{zear}) is the only available conditional gene expression system for *F. graminearum* (Lee et al. 2010). Furthermore, the potential for the inexpensive reagent β-estradiol (β-est) to substitute for ZEA in this conditional gene expression system has been demonstrated, thereby facilitating the utilization of this system in high-throughput studies (Lee et al. 2011).

We generated HK226 strains in which the promoter of the *FgHSP90* gene was replaced with P_{zear} and confirmed the preciseness of this genetic manipulation using Southern blot analysis (Fig. 2b). HK226 mutant strains displayed dramatically reduced transcript levels of *FgHSP90* (Fig. 2c) and severely defective mycelial growth compared to the wild-type strain (Fig. 2d). Adding β-est partially restored radial growth and reduced the transcript level of *FgHSP90*.

These results indicated that the P_{zear} system is applicable to this study. There was no apparent difference in mycelial morphology between the HK226 mutant and wild-type strains (data not shown).

To examine the requirement of *FgHSP90* for heat shock adaptation, heat shock (48 °C for 30 min) was applied to both the HK226 mutant and wild-type strains. Most HK226 mutant strains were inviable after heat shock treatment, whereas the wild-type strain exhibited slightly delayed radial growth (Table 5 and Fig. 2d). When β-est was applied, the two heat shock-treated strains grew similarly. The germination rate of serial dilution assays confirmed that most of HK226 mutant conidia were blocked to germinate after heat shock treatment, whereas the growth rate of wild-type strain were only retarded (Fig. 2e). Adding β-est partly restored the growth and viability of HK226 mutants. We also examined the sensitivity of the HK226 mutant strains to various stress conditions, including osmotic and oxidative stresses, cell wall-damaging agent exposure, fungicide exposure, and altered pH. None of these stress conditions altered the growth of HK226 mutant strains (Fig. 4).

Table 5. Vegetative growth, conidial production and morphology, and virulence of the *FgHSP90*-repressed mutants. Radial growth was measured 3 days after inoculation. Conidia were harvested from a 1-day-old culture in yeast malt agar. The disease index (number of diseased spikelets per wheat head) of the strains was measured 21 days after inoculation. CM, complete medium; β-est, β-estradiol; *, data differed significantly ($P < 0.05$) based on Tukey's test within each column; Z-3639, *F. graminearum* wild-type strain; HK226, *F. graminearum FgHSP90*-repressed strains.

Strain	Radial growth (mm)		Conidial morphology						Virulence (disease index)	
	CM	CM β-est	CM			CM β-est			-	β-est
			Length (μm)	Width (μm)	No. of septa	Length (μm)	Width (μm)	No. of septa		
Z-3639	63.5	48.6	53.0	5.8	4.5	54.5	5.8	4.7	11.5	9.1
HK226-6	12.6*	34.6*	62.6*	5.5*	4.9*	60.6*	5.7	5.0*	0.7*	0.6*
HK226-8	10.8*	33.1*	65.5*	5.6*	4.9*	64.8*	6.1	5.0*	0.6*	0.9*

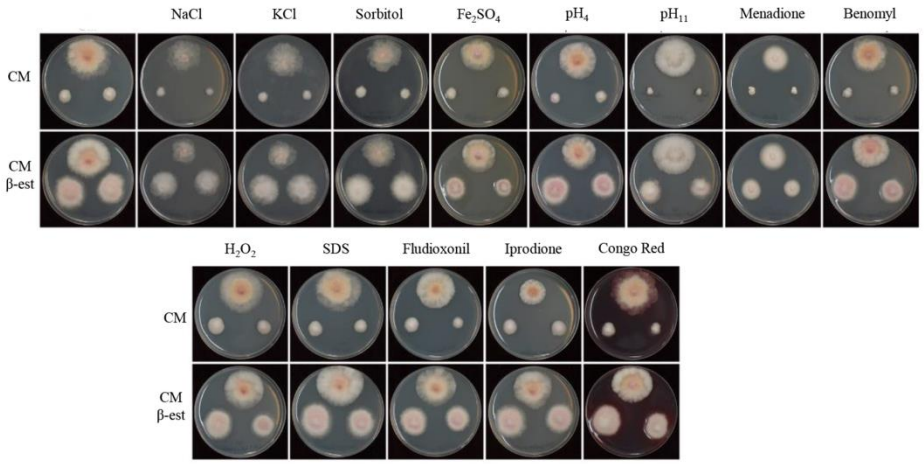

Figure 4. The observation of various stresses response in the repression of *FgHSP90* mutants (HK226). The pictures were taken at 3 days after inoculation.

V. *FgHSP90* is required for conidiation in *F. graminearum*

Genetic repression of *FgHSP90* resulted in severe defects in asexual sporulation. First, conidial production by the HK226 strains was markedly reduced compared to that by the wild-type strain, but supplementation with β-est partially restored defective conidiation by the HK226 strains (Fig. 5a). Furthermore, the conidial morphologies of the HK226 strains were significantly altered. The conidia of the HK226 strains tended to be longer and thinner than those of the wild-type strain. HK226 conidia had more septa than wild-type conidia; this difference was observed due to the occurrence of conidia with 6 ~ 8 septa in the HK226 strains (Table 5 and Fig. 5b,c).

To gain further insight into the role of *FgHSP90* in the asexual sporulation process in *F. graminearum*, we observed conidiophore morphogenesis at the microscopic level. To visualize nuclei, the HK301 strains (P_{zear}-*FgHSP90 hH1-GFP-HYG*) were generated by outcrossing the mat1g and HK226 strains (Table 1). The hH1-GFP strain, carrying the wild-type allele of *FgHSP90*, initially produced phialides from the hyphae, and conidia were subsequently formed from mature phialides (Fig. 5e). In addition, conidia were often directly produced from hyphae. However, genetic repression of *FgHSP90* abolished phialide formation, and consequently, most conidia were directly produced from hyphae or at the hyphal tips (arrowheads in Fig. 5e). Phialide

production by the HK301 mutant strains was partly restored by supplementing the cultures with β-est (arrows in Fig. 5e).

We further investigated the possible link between *FgHSP90* and representative conidiation-related genes in the wild-type and HK226 strains. The transcript levels of five genes, *STUA* (Lysøe et al. 2011), *HTF1* (Zheng et al. 2012), *REN1* (Ohara et al. 2004), *ABAA* (Son et al. 2013), and *WETA* (Son et al. 2014), were significantly decreased in the HK226 mutant strains compared to the wild-type strain (Fig. 5d). Although the expression levels of *ABAA* and *WETA*, transcription factors specifically involved in conidiogenesis in *F. graminearum* (Son et al. 2013; Son et al. 2014), were generally undetectable in the HK226 mutant strains (Fig. 5d), the HK305 (Δ*abaA* P_{zear}-*FgHSP90*) strains (Table 1) could not produce conidia in either YMA or CMC medium (data not shown).

To further confirm the necessity of AbaA for conidiation, we next visualized the localization of this protein during the conidiation stage. As noted in a previous report (Son et al. 2013), AbaA-Gfp was highly accumulated in the phialides and in the nuclei of terminal cells of maturing conidia in AbaAc strains (Fig. 5f). The expression of AbaA-Gfp in the HK306 (*ABAA-GFP* P_{zear}-*FgHSP90*) strains showed an identical pattern (Fig. 5f). The conidial germination rates of the HK226 mutant strains were similar to those of the wild-type strain,

whereas *HSP90*-repressed *A. fumigatus* mutant strains showed retarded conidial germination (Lamoth et al. 2012). These findings suggest that *FgHSP90* is dispensable for germination in *F. graminearum*.

VI. *FgHSP90* is involved in virulence and sexual development

To determine the role of *FgHSP90* in pathogenicity, we performed a virulence assay on flowering wheat heads by point inoculation. The wild-type strain caused typical head blight symptoms 21 days after inoculation as expected, whereas the HK226 strains were unable to spread from the inoculated spikelet to adjacent spikelets on the heads (Table 5 and Fig. 6a). In contrast to its effects on the growth rate and conidiation, supplementation with β-est did not restore the virulence of the HK226 mutant strains.

To further visualize the movement of mycelia during infection of wheat heads at the microscopic level, we generated HK302 (P_{zear}-*FgHSP90 GFP-HYG*) strains by outcrossing the KM19 (Δ*mat1::GEN GFP-HYG*, constitutively expressing green fluorescent protein [Gfp]) and HK226 strains (Table 1). The HK12 strain, carrying the wild-type allele of *FgHSP90*, spread hyphae to the adjacent spikelet through its rachis node (Fig. 6b). The hyphae of HK302 strains were observed only at the inoculated points of the rachis, and these strains failed to colonize the injected spikelet and spread to the adjacent spikelet (Fig. 6b).

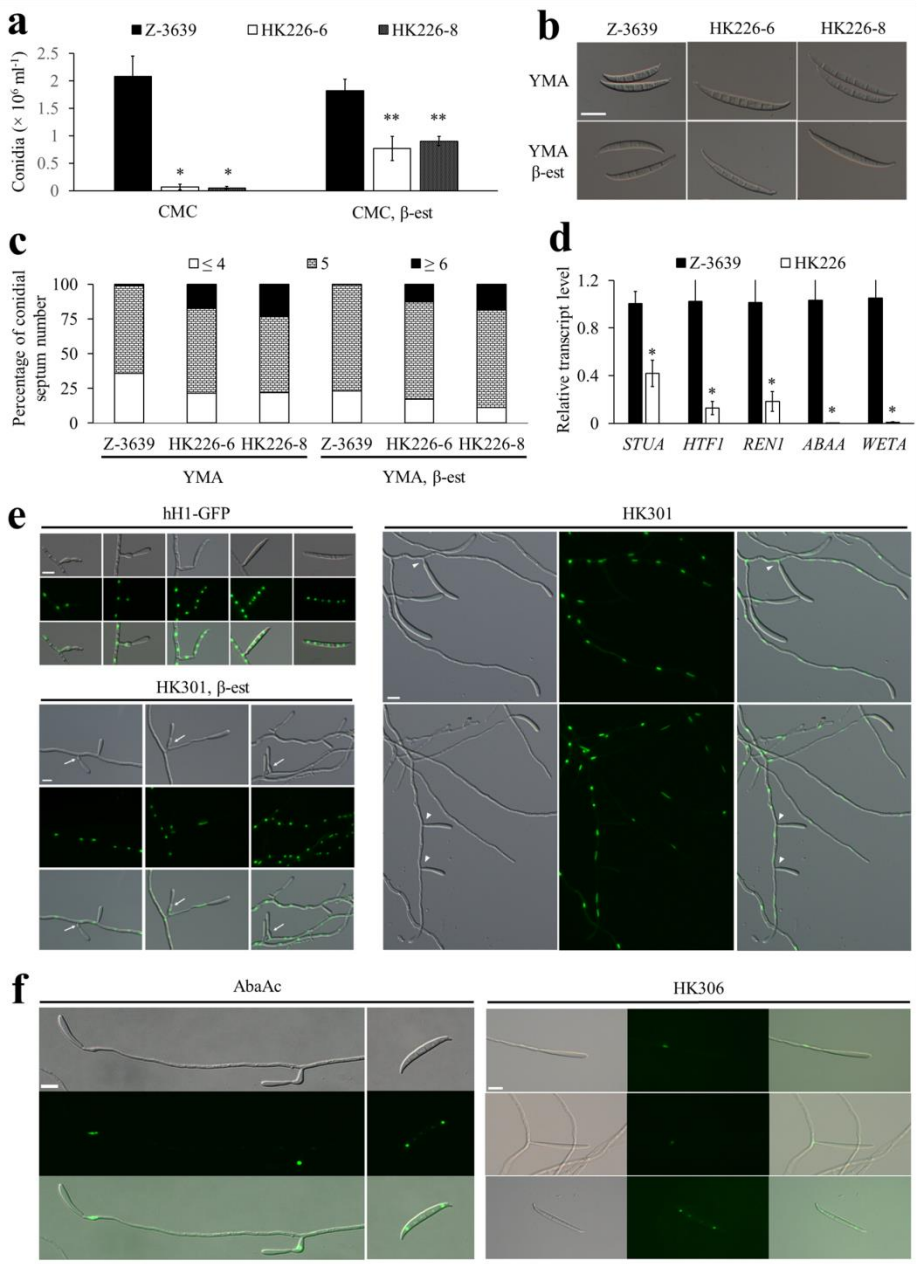

Figure 5. Conidiation in the repression of *FgHSP90* mutants. (**a**) Conidial production. The number of conidia was counted after 5 days of incubation in CMC in the absence or presence of β-est. The values were generated based on three biological replicates. (**b**) Conidial morphology. Conidia were induced on YMA in the absence or presence

of β-est and subsequently observed by DIC microscopy. Scale bar = 20 μm. (**c**) Percentage of conidial septa. One hundred conidia induced on YMA were assessed for each strain with three biological replicates. (**d**) Relative transcript levels of genes related to conidiation. Total RNA was extracted from the wild-type and HK226 strains cultured in CM for 48 h and then subjected to asexual induction in CMC for 6 h. The relative transcript levels of each gene in the wild-type strain were arbitrarily set to 1. (**e**) Morphology of conidiophores in *F. graminearum* strains. Images were captured 1 to 3 days after conidial induction on CMC in the absence or presence of β-est. Arrows and arrowheads indicate phialides and conidia directly produced from hyphae, respectively. Scale bar = 10 μm. (**f**) Cellular localization of AbaA-Gfp in the strain with wild-type allele of *FgHSP90* (left) and in the *FgHSP90*-repressed strain (right). Scale bar = 10 μm.

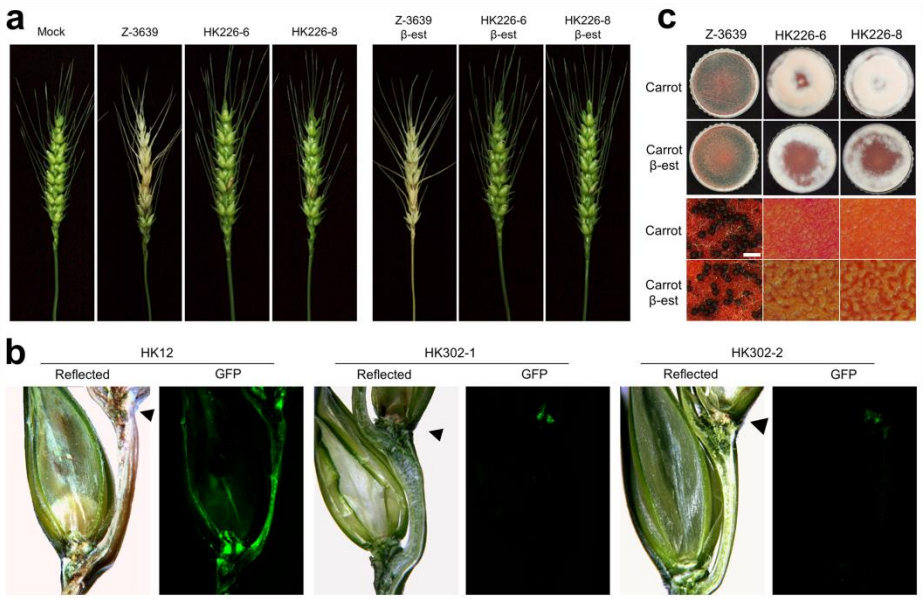

Figure 6. Virulence and sexual development. (**a**) Virulence on wheat heads. The centre spikelet of each wheat head was injected with 10 µl of a conidial suspension. Images were captured 21 days after inoculation. (**b**) Micrographs of manually generated sections after infection of wheat. Wheat spikelets were inoculated with conidial suspensions from strains expressing Gfp in the cytoplasm (HK12 and HK302). Infected wheat heads were longitudinally dissected 6 days after inoculation and examined under a fluorescence microscope. Gfp fluorescence represents hyphae spreading from the inoculation points. Arrowheads mark the inoculated spikelets. Reflected, reflected light. (**c**) Sexual development. A five-day-old culture in carrot agar was mock-fertilized to induce sexual production and incubated for an additional 7 days. The upper and below panels show photographs of

self-fertility on a whole carrot agar plate and photographs captured using a dissecting microscope, respectively. Scale bar = 500 μm.

We next examined the role of *FgHSP90* in sexual development. The wild-type strain began to produce detectable perithecial initials 3 days after sexual induction, and mature perithecia were subsequently produced after an additional 3 or 4 days of incubation (Fig. 6c). In contrast to the wild-type strain, repressing *FgHSP90* completely blocked the production of perithecia even in the presence of β-est (Fig. 6c).

VII. The subcellular localization pattern of *Fg*Hsp90 reveals its multiple functions during the conidiation stage

To examine the subcellular localization of *Fg*Hsp90 during the developmental stages of *F. graminearum*, the HK227 strains expressing the *Fg*Hsp90-Gfp fusion protein were generated (Fig. 7). Dozens of transformants containing a single copy of *FgHSP90-GFP* were obtained, and nuclear Gfp fluorescent signals were observed in these strains. For confirmation of the nuclear localization of *Fg*Hsp90, HK303 (*FgHSP90-GFP-HYG hH1-RFP-HYG*) strains were generated by outcrossing the HK227 strain and the mat1r strain, which carries a gene encoding red fluorescent protein (Rfp) fused to the histone H1 protein in a *MAT1-1* deletion background.

We next investigated the localization patterns of *Fg*Hsp90 in hyphae and conidiophores under optimal and heat shock conditions.

Interestingly, a distinct shift in Gfp signals from the cytosol to the nuclei was observed after heat shock treatment at 37 °C (Fig. 8a,b). Similarly, an in-depth examination of Hsp90 localization during conidiogenesis showed that *Fg*Hsp90 was highly accumulated in the nuclei of mature phialides and conidia (Fig. 8b); this expression pattern corresponds to the functions of *Fg*Hsp90 in the late stages of conidiation. *Fg*Hsp90 was evenly distributed throughout the cytoplasm after conidial germination (Fig. 8c). Distinct nuclear localization of *Fg*Hsp90 was not observed in ascospores (sexually produced spores) (Fig. 8c). However, germination rate and viability of conidia and ascospores under heat shock stress were indistinguishable (Fig. 9).

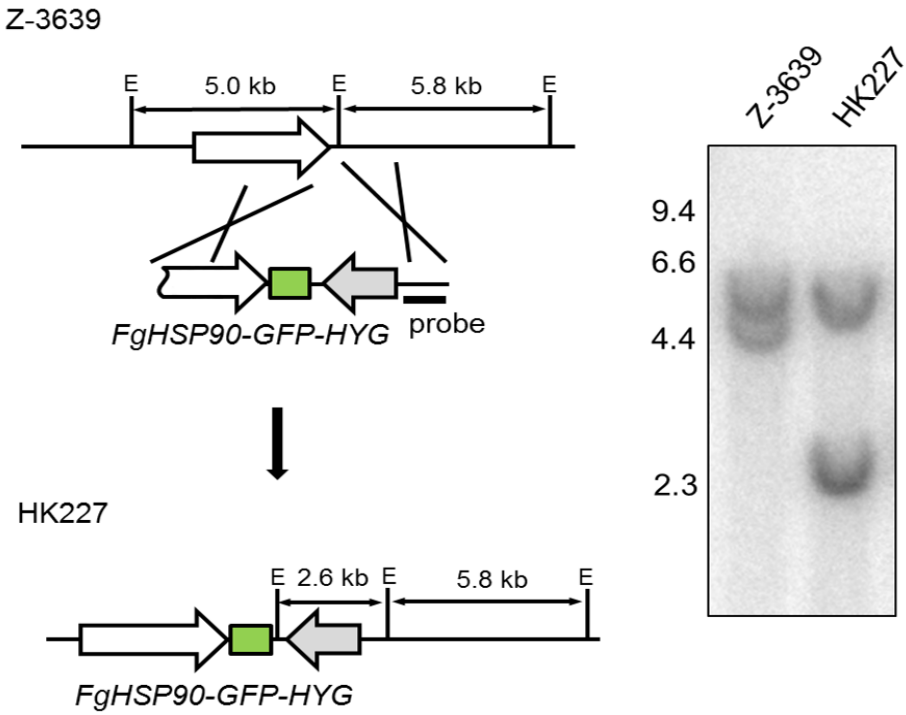

Figure 7. Schematic illustrating the strategy for fusion of Gfp to *Fg*Hsp90. Left panel: Strategy used to fuse *GFP* to the 3′ end of *FgHSP90*. Right panel: Southern blot analysis confirming genetic construct. Lane 1, wild-type Z-3639 strain; Lane 2, *FgHSP90-GFP* strain (HK227). Sizes of the DNA standards (kb) are indicated to the left of the blot. E, EcoRV.

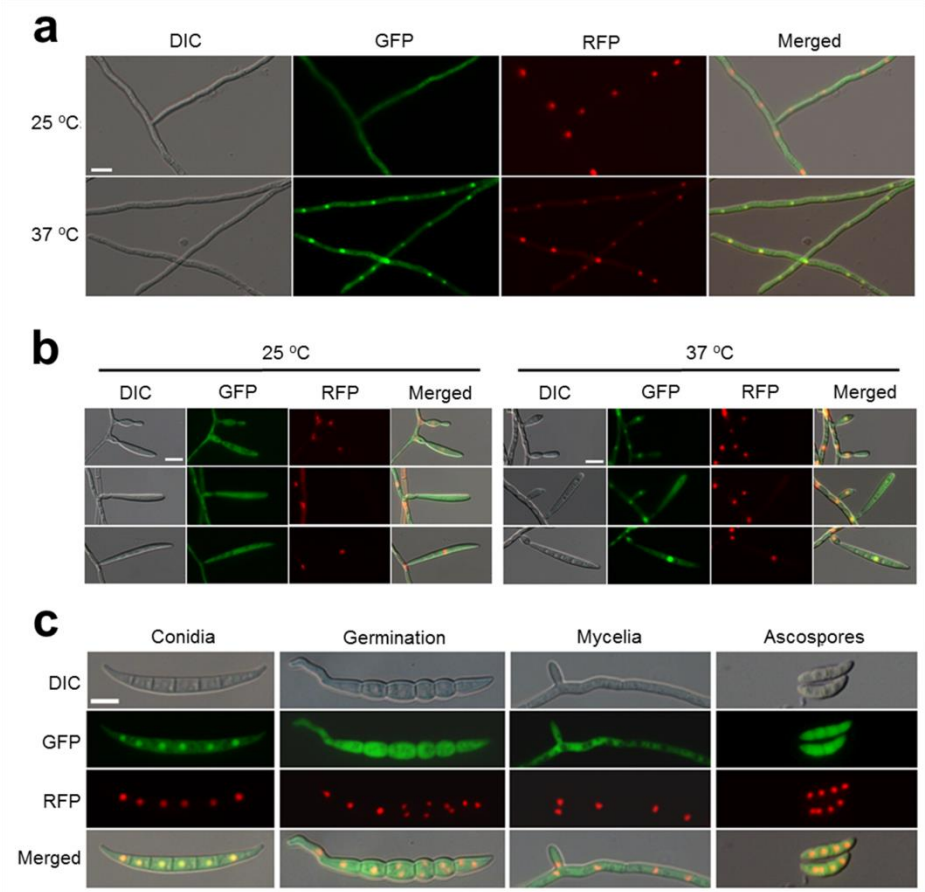

Figure 8. Localization of *Fg*Hsp90 in *F. graminearum*. Representative images showing co-localization of *Fg*Hsp90 fused to Gfp with histone H1 fused to Rfp. (**a**) *Fg*Hsp90 translocated to nuclei from the cytosol after heat shock treatment at 37 °C for 1 h. Scale bar = 10 µm. (**b**) Localization of *Fg*Hsp90 during conidiogenesis in CMC under optimal conditions (left) and heat shock treatment (37 °C for 1 h) (right). Scale bar = 10 µm. (**c**) A strain containing *FgHSP90-GFP* and *hH1-RFP* was grown on YMA (conidia), CM (germination and mycelia), or carrot agar medium (ascospores) for microscopic observation. DIC, differential interference contrast. Scale bar = 10 µm.

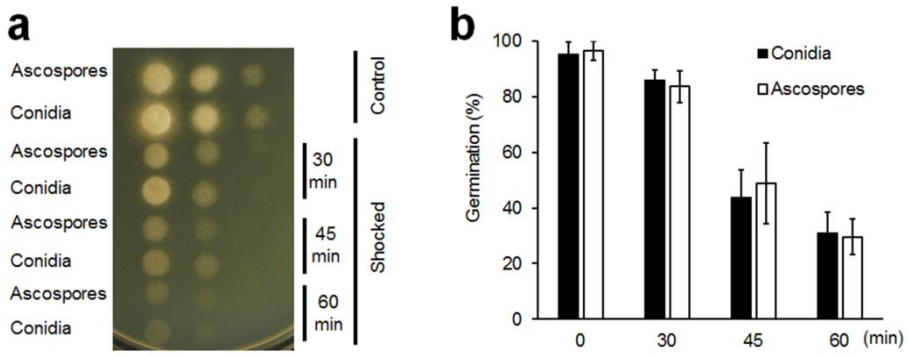

Figure 9. Heat shock response of the sexual and asexual spores in *F. graminearum*. (**a**) Serial dilutions of wild-type conidia and ascospores were point-inoculated onto CM medium. The heat shock treatment was conducted at 42 ^{o}C for 30, 45, and 60 min, respectively. (**b**) Germination assay. Germination rate was measured from optimal and heat shock treatment assays 12 h after inoculation. One hundred conidia were assessed for each strain with three biological replicates.

DISCUSSION

In this study, the heat shock response in the plant pathogenic fungus *F. graminearum* was investigated for the first time using transcriptome analysis. The heat shock response accompanied a dramatic alteration in the gene expression profile in *F. graminearum*. In particular, we identified the heat shock protein *Fg*Hsp90, which appeared to play the prominent roles in response to thermal stress. In-depth functional analyses revealed that *Fg*Hsp90 also performs crucial functions in *F. graminearum* during various developmental stages including vegetative growth, asexual and sexual reproduction, and virulence. Moreover, subcellular localization patterns supported that *Fg*Hsp90 performs multiple functions as a transcriptional regulator as well as a chaperone during conidiation. Taken together, the results of our study shed light into the roles of the heat shock protein Hsp90 in fungal development.

Hsp90 is a conserved molecular chaperone that functions in the refolding of denatured and/or aggregated proteins generated by high temperature stress (Jackson 2013). We found that *Fg*Hsp90 plays the most active role in the response to heat stress in *F. graminearum* compared to other genes related to responses to temperature (Table 4). Moreover, the orthologue for the Hsp90 co-chaperone Sti1 was also highly expressed under thermal stress conditions. StiA (a homologue of

Sti1 in *A. fumigatus*) is not required for the physical interaction between Hsp70 and Hsp90 but does play distinct roles in the regulation of Hsp90 by inhibiting ATPase activity (Lee et al. 2012; Lamoth et al. 2015). Taken together, this evidence indicates that *Fg*Hsp90 and related regulatory pathways play key roles in thermotolerance in *F. graminearum*.

Our study confirmed that *FgHSP90* is an essential gene that performs diverse functions in fungal development and virulence. In *C. albicans*, *Ca*Hsp90 functions as a regulator of morphology by repressing Ras/PKA pathway (Shapiro et al. 2009), and *Ca*Hsp90 is required for virulence (Cowen et al. 2009). *Af*Hsp90 of *A. fumigatus* is involved in spore viability, hyphal growth, conidiation and virulence (Lamoth et al. 2012; Lamoth et al. 2014a). Similarly, repression of *FgHSP90* resulted in pleiotropic phenotypic defects including deficiencies in morphogenesis and virulence, and these observations support the conserved roles of Hsp90 among fungi. However, the involvement of Hsp90 in sexual development was first reported in *F. graminearum*. In addition, although *AfHSP90* plays a crucial role in the regulation of cell wall integrity pathways in *A. fumigatus* (Lamoth et al. 2012), *FgHSP90* repression led to wild-type phenotypes under various stress conditions including exposure to cell wall-damaging agents. Taken together, these results indicate that Hsp90s play highly conserved roles in the fungal kingdom but that some differences in their function

between species might be attributed to different physiologies among fungi and variations in regulatory mechanisms of Hsp90 at the post-translational level.

AfHSP90 repression induces a defect in asexual sporulation, affecting both the production and pigmentation of conidia, and this defect is associated with downregulation of the conidiation-specific genes *BRLA*, *WETA* and *ABAA* (Lamoth et al. 2012). Similarly, our in-depth examination of Hsp90 function in *F. graminearum* verified its specific role in asexual sporulation. *FgHSP90* was highly expressed during conidiogenesis and participated in the formation of conidiogenous cells, referred to as phialides, by upregulating conidiation-specific genes (*STUA*, *HTF1*, *REN1*, *ABAA*, and *WETA*). Moreover, *Fg*Hsp90 was highly accumulated in nuclei at the late stage of conidiophores and conidia, and this localization pattern suggests a role of *Fg*Hsp90 as a transcriptional regulator specifically involved in conidiation. Specific nuclear localization of Hsp90 orthologues during conidiation has not been reported in other organisms, although stress conditions commonly induce nuclear localization of Hsp90 (Lamoth et al. 2012).

In conclusion, this study revealed the key roles of *Fg*Hsp90 in heat shock responses and fungal development via genome-wide transcriptome analysis in the plant pathogenic fungus *F. graminearum*.

Comprehensive functional characterization of *Fg*Hsp90 demonstrated that *Fg*Hsp90 performs crucial functions in vegetative growth, reproduction, and virulence. We also produced evidence that *Fg*Hsp90 performs multiple functions as a transcriptional regulator as well as a chaperone for conidiation. The results of this study provide new insight into the mechanistic roles of Hsp90 in fungal development and virulence.

LITERATURE CITED

Ba ANN, Pogoutse A, Provart N, Moses AM. 2009. NLStradamus: a simple Hidden Markov Model for nuclear localization signal prediction. *BMC Bioinformatics* **10**: 202.

Baldwin TK, Urban M, Brown N, Hammond-Kosack KE. 2010. A role for topoisomerase I in *Fusarium graminearum* and *F. culmorum* pathogenesis and sporulation. *Mol Plant-Microbe Interact* **23**: 566-577.

Barrett T, Wilhite SE, Ledoux P, Evangelista C, Kim IF, Tomashevsky M, Marshall KA, Phillippy KH, Sherman PM, Holko M. 2013. NCBI GEO: archive for functional genomics data sets - update. *Nucleic Acids Res* **41**: D991-D995.

Borkovich K, Farrelly F, Finkelstein D, Taulien J, Lindquist S. 1989. hsp82 is an essential protein that is required in higher concentrations for growth of cells at higher temperatures. *Mol Cell Biol* **9**: 3919-3930.

Bowden RL, Leslie JF. 1999. Sexual recombination in *Gibberella zeae*. *Phytopathology* **89**: 182-188.

Cappellini R, Peterson J. 1965. Macroconidium formation in submerged cultures by a non-sporulating strain of *Gibberella zeae*. *Mycologia*: 962-966.

Colot HV, Park G, Turner GE, Ringelberg C, Crew CM, Litvinkova L, Weiss RL, Borkovich KA, Dunlap JC. 2006. A high-throughput

gene knockout procedure for *Neurospora* reveals functions for multiple transcription factors. *Proc Natl Acad Sci U S A* **103**: 10352-10357.

Cowen LE, Lindquist S. 2005. Hsp90 potentiates the rapid evolution of new traits: Drug resistance in diverse fungi. *Science* **309**: 2185-2189.

Cowen LE, Singh SD, Köhler JR, Collins C, Zaas AK, Schell WA, Aziz H, Mylonakis E, Perfect JR, Whitesell L. 2009. Harnessing Hsp90 function as a powerful, broadly effective therapeutic strategy for fungal infectious disease. *Proc Natl Acad Sci U S A* **106**: 2818-2823.

Cutforth T, Rubin GM. 1994. Mutations in *Hsp83* and *cdc37* impair signaling by the sevenless receptor tyrosine kinase in Drosophila. *Cell* **77**: 1027-1036.

Desjardins A. 2006. *Fusarium mycotoxins: chemistry, genetics and biology*. St Paul, MN, USA: American Phytopathology Society St Paul, MN, USA: American Phytopathology Society

Harris SD. 2005. Morphogenesis in germinating *Fusarium graminearum* macroconidia. *Mycologia* **97**: 880-887.

Hendrick JP, Hartl F-U. 1993. Molecular chaperone functions of heat-shock proteins. *Annu Rev Biochem* **62**: 349-384.

Hodgetts S, Matthews R, Morrissey G, Mitsutake K, Piper P, Burnie J. 1996. Over-expression of *Saccharomyces cerevisiae* hsp90

enhances the virulence of this yeast in mice. *FEMS Immunol Med Microbiol* **16**: 229-234.

Hong S-Y, So J, Lee J, Min K, Son H, Park C, Yun S-H, Lee Y-W. 2010. Functional analyses of two syntaxin-like SNARE genes, *GzSYN1* and *GzSYN2*, in the ascomycete *Gibberella zeae*. *Fungal Genet Biol* **47**: 364-372.

Horwitz BA, Sharon A, Lu S-W, Ritter V, Sandrock TM, Yoder O, Turgeon BG. 1999. A G protein alpha subunit from *Cochliobolus heterostrophus* involved in mating and appressorium formation. *Fungal Genet Biol* **26**: 19-32.

Imai J, Yahara I. 2000. Role of HSP90 in salt stress tolerance via stabilization and regulation of calcineurin. *Mol Cell Biol* **20**: 9262-9270.

Imazu H, Sakurai H. 2005. *Saccharomyces cerevisiae* heat shock transcription factor regulates cell wall remodeling in response to heat shock. *Eukaryot Cell* **4**: 1050-1056.

Jackson SE. 2013. Hsp90: structure and function. *Top Curr Chem* **328**: 155-240.

Johnson JL. 2012. Evolution and function of diverse Hsp90 homologs and cochaperone proteins. *Biochim Biophys Acta* **1823**: 607-613.

Kazan K, Gardiner DM, Manners JM. 2012. On the trail of a cereal killer: recent advances in *Fusarium graminearum*

pathogenomics and host resistance. *Mol Plant Pathol* **13**: 399-413.

Kim H-K, Yun S-H. 2011. Evaluation of potential reference genes for quantitative RT-PCR analysis in *Fusarium graminearum* under different culture conditions. *Plant Pathology J* **27**: 301-309.

Lamoth F, Juvvadi PR, Fortwendel JR, Steinbach WJ. 2012. Heat shock protein 90 is required for conidiation and cell wall integrity in *Aspergillus fumigatus*. *Eukaryot Cell* **11**: 1324-1332.

Lamoth F, Juvvadi PR, Gehrke C, Asfaw YG, Steinbach WJ. 2014a. Transcriptional activation of heat shock protein 90 mediated via a proximal promoter region as trigger of caspofungin resistance in *Aspergillus fumigatus*. *J Infect Dis* **209**: 473-481.

Lamoth F, Juvvadi PR, Steinbach WJ. 2014b. Heat shock protein 90 (Hsp90): a novel antifungal target against *Aspergillus fumigatus*. *Crit Rev Microbiol*.

Lamoth F, Juvvadi PR, Soderblom EJ, Moseley MA, Steinbach WJ. 2015. Hsp70 and the cochaperone StiA (Hop) orchestrate Hsp90-mediated caspofungin tolerance in *Aspergillus fumigatus*. *Antimicrob Agents Chemother* **59**: 4727-4733.

Lee CT, Graf C, Mayer FJ, Richter SM, Mayer MP. 2012. Dynamics of the regulation of Hsp90 by the co-chaperone Sti1. *EMBO J* **31**: 1518-1528.

Lee J, Lee T, Lee YW, Yun SH, Turgeon BG. 2003. Shifting fungal

reproductive mode by manipulation of mating type genes: obligatory heterothallism of *Gibberella zeae*. *Mol Microbiol* **50**: 145-152.

Lee J, Son H, Lee S, Park AR, Lee Y-W. 2010. Development of a conditional gene expression system using a zearalenone-inducible promoter for the ascomycete fungus *Gibberella zeae*. *Appl Environ Microbiol* **76**: 3089-3096.

Lee J-K, Son H-K, Lee Y-W. 2011. Estrogenic compounds compatible with a conditional gene expression system for the phytopathogenic fungus *Fusarium graminearum*. *Plant Pathology J* **27**: 349-353.

Leslie JF, Summerell BA, Bullock S. 2006. *The Fusarium laboratory manual*. Wiley-Blackwell, 2121 State Avenue, Ames, Iowa 50014, USA.

Livak KJ, Schmittgen TD. 2001. Analysis of relative gene expression data using real-time quantitative PCR and the $2^{-\Delta\Delta CT}$ method. *Methods* **25**: 402-408.

Loubradou G, Bégueret J, Turcq B. 1997. A mutation in an *HSP90* gene affects the sexual cycle and suppresses vegetative incompatibility in the fungus *Podospora anserina*. *Genetics* **147**: 581-588.

Lysøe E, Pasquali M, Breakspear A, Kistler HC. 2011. The transcription factor FgStuAp influences spore development,

pathogenicity, and secondary metabolism in *Fusarium graminearum*. *Mol Plant-Microbe Interact* **24**: 54-67.

Min K, Son H, Lee J, Choi GJ, Kim J-C, Lee Y-W. 2012. Peroxisome function is required for virulence and survival of *Fusarium graminearum*. *Mol Plant-Microbe Interact* **25**: 1617-1627.

Mortazavi A, Williams BA, McCue K, Schaeffer L, Wold B. 2008. Mapping and quantifying mammalian transcriptomes by RNA-Seq. *Nat Methods* **5**: 621-628.

Nathan DF, Vos MH, Lindquist S. 1997. *In vivo* functions of the *Saccharomyces cerevisiae* Hsp90 chaperone. *Proc Natl Acad Sci U S A* **94**: 12949-12956.

Ohara T, Inoue I, Namiki F, Kunoh H, Tsuge T. 2004. *REN1* is required for development of microconidia and macroconidia, but not of chlamydospores, in the plant pathogenic fungus *Fusarium oxysporum*. *Genetics* **166**: 113-124.

Picard D, Khursheed B, Garabedian MJ, Fortin MG, Lindquist S, Yamamoto KR. 1990. Reduced levels of hsp90 compromise steroid receptor action *in vivo*. *Nature* **348**: 166-168.

Richter K, Haslbeck M, Buchner J. 2010. The heat shock response: life on the verge of death. *Mol Cell* **40**: 253-266.

Rowley A, Johnston G, Butler B, Werner-Washburne M, Singer R. 1993. Heat shock-mediated cell cycle blockage and G1 cyclin expression in the yeast *Saccharomyces cerevisiae*. *Mol Cell Biol*

13: 1034-1041.

Sambrook J, Russell D. 2001. *Molecular cloning: a laboratory manual*. Cold Spring Harbor Laboratory Press, Cold Spring Harbor, NY, USA.

Shapiro RS, Uppuluri P, Zaas AK, Collins C, Senn H, Perfect JR, Heitman J, Cowen LE. 2009. Hsp90 orchestrates temperature-dependent *Candida albicans* morphogenesis via Ras1-PKA signaling. *Curr Biol* **19**: 621-629.

Son H, Lee J, Park AR, Lee Y-W. 2011a. ATP citrate lyase is required for normal sexual and asexual development in *Gibberella zeae*. *Fungal Genet Biol* **48**: 408-417.

Son H, Min K, Lee J, Raju NB, Lee Y-W. 2011b. Meiotic silencing in the homothallic fungus *Gibberella zeae*. *Fungal Biol* **115**: 1290-1302.

Son H, Kim M-G, Min K, Seo Y-S, Lim JY, Choi GJ, Kim J-C, Chae S-K, Lee Y-W. 2013. AbaA regulates conidiogenesis in the ascomycete fungus *Fusarium graminearum*. *PloS One* **8**: e72915.

Son H, Kim M-G, Min K, Lim JY, Choi GJ, Kim J-C, Chae S-K, Lee Y-W. 2014. WetA is required for conidiogenesis and conidium maturation in the ascomycete fungus *Fusarium graminearum*. *Eukaryot Cell* **13**: 87-98.

Trail F, Gaffoor I, Vogel S. 2005. Ejection mechanics and trajectory of

the ascospores of *Gibberella zeae* (anamorph *Fuarium graminearum*). *Fungal Genet Biol* **42**: 528-533.

Vidair C, Huang R, Doxsey S. 1996. Heat shock causes protein aggregation and reduced protein solubility at the centrosome and other cytoplasmic locations. *Int J Hyperther* **12**: 681-695.

Wong P, Walter M, Lee W, Mannhaupt G, Münsterkötter M, Mewes H-W, Adam G, Güldener U. 2011. FGDB: revisiting the genome annotation of the plant pathogen *Fusarium graminearum*. *Nucleic Acids Res* **39**: D637-D639.

Yu J-H, Hamari Z, Han K-H, Seo J-A, Reyes-Domínguez Y, Scazzocchio C. 2004. Double-joint PCR: a PCR-based molecular tool for gene manipulations in filamentous fungi. *Fungal Genet Biol* **41**: 973-981.

Zheng W, Zhao X, Xie Q, Huang Q, Zhang C, Zhai H, Xu L, Lu G, Shim W-B, Wang Z. 2012. A conserved homeobox transcription factor Htf1 is required for phialide development and conidiogenesis in *Fusarium* species. *PloS One* **7**: e45432.

CHAPTER 2

The *Fg*Not3 subunit of the Ccr4-Not complex regulates vegetative growth, sporulation, and virulence in *Fusarium graminearum*

ABSTRACT

The Ccr4-Not complex is evolutionarily conserved and important for multiple cellular functions in eukaryotic cells. In this study, the biological roles of the *Fg*Not3 subunit of this complex were investigated in the plant pathogenic fungus *Fusarium graminearum*. Deletion of *FgNOT3* resulted in retarded vegetative growth and spore germination, swollen hyphae, and hyper-branching. The Δ*Fgnot3* mutants also showed impaired sexual and asexual sporulation, decreased virulence, and reduced expression of genes related to conidiogenesis. *Fgnot3* deletion mutants were sensitive to thermal stress, whereas *NOT3* orthologs in other model eukaryotes are known to be required for cell wall integrity. We found that *Fg*Not3 functions as a negative regulator of the production of secondary metabolites, including trichothecenes and zearalenone. Additionally, the alteration of transcript levels of all Not subunits in the absence of *FgNOT3* and the numerous defects in deletion mutants of *FgNOT2* and *FgNOT4* demonstrated that the Not module of the Ccr4-Not complex is conserved, and each subunit not only primarily functions within the context of a complex, but also might have distinct roles outside of the complex in *F. graminearum*. This is the first study to functionally characterize the Not module in filamentous fungi and provides novel insights into signal transduction pathways in fungal development.

INTRODUCTION

Fusarium graminearum is an ascomycetous fungus that causes *Fusarium* head blight in cereal crops worldwide, including wheat, barley, and rice, as well as ear and stalk rot in maize (Sutton 1982; Goswami and Kistler 2004). Fungal infection of *F. graminearum* leads to yield and quality losses as well as contamination of grains by the production of mycotoxins (trichothecenes and zearalenone) that threaten human and animal health (Desjardins 2006). *F. graminearum* produces both sexual (ascospores) and asexual (conidia) spores (Leslie et al. 2006). Ascospores are produced and discharged from the perithecia during flowering and function as primary inocula (Sutton 1982; Guenther and Trail 2005). The initial structures or associated hyphae of the perithecia also serve as survival structures for overwintering (Sutton 1982; Guenther and Trail 2005). Conidia are responsible for secondary infections that are produced from sporodochia present on infected crops (Guenther and Trail 2005). The biological processes of sexual and asexual sporulation in *F. graminearum* are under precise temporal and spatial regulation related to various cellular processes (Ohara et al. 2004; Lysoe et al. 2011; Son et al. 2011b; Zheng et al. 2012; Son et al. 2013; Son et al. 2014).

The Ccr4-Not complex is an evolutionarily conserved multi-subunit complex required for numerous cellular processes (Collart and

Panasenko 2012). Decades of studies on model eukaryotes have revealed that the Ccr4-Not complex regulates multiple nuclear and cytoplasmic steps in gene expression, such as transcription initiation, mRNA elongation and degradation, translation, and protein degradation (Collart 2003; Goldstrohm and Wickens 2008; Collart and Panasenko 2012; Miller and Reese 2012; Collart et al. 2013). In *Saccharomyces cerevisiae*, the complex consists of nine proteins, including five *Sc*Not proteins, three *Sc*Caf proteins, and one *Sc*Ccr4 protein (Bai et al. 1999; Maillet et al. 2000). The *Sc*Not proteins (*Sc*Not1-5) are negative regulators of genes lacking a canonical TATA box (Collart and Struhl 1994). The *ScCCR4* (carbon catabolite repression) gene positively regulates glucose-repressible enzymes (Denis 1984). The *Sc*Caf (*Sc*Ccr4 associated factor) proteins, *Sc*Caf1 (also known as *Sc*Pop2), *Sc*Caf40, and *Sc*Caf130, physically interact with *Sc*Ccr4 (Draper et al. 1995; Chen et al. 2001). Other proteins, including *Sc*Caf4, *Sc*Caf16, *Sc*Dhh1, and *Sc*Btt1, have also been shown to associate with the core of the Ccr4-Not complex (Collart 2003). In human cells, two genes (*CNOT7* and *CNOT8*) are orthologous to yeast *ScCAF1*, and *Sc*Ccr4 orthologs are also encoded by separated genes, *CNOT6* and *CNOT6L* (Collart and Timmers 2004). In contrast, there is only one gene (*CNOT3*) ortholog for yeast *ScNOT3* and *ScNOT5*, which likely originated from a gene duplication event in yeast.

Yeast *ScNOT5* is involved in diverse cellular processes, including maintaining cell wall integrity, carbon catabolite repression, and filamentation (Oberholzer and Collart 1998; Collart 2003), and has recently been identified as an essential cellular regulator linking transcription, mRNA degradation, and translation (Villanyi et al. 2014). *CaNOT5* is important in morphogenesis and virulence (Cheng et al. 2005), and deletion of *CaNOT5* affected cell wall structure and adherence properties in *Candida albicans* (Jin et al. 2008). In humans, *CNOT3* is an important regulator of biological processes such as retinal homeostasis, heart physiology, and stem cell self-renewal (Hu et al. 2009; Neely et al. 2010; Venturini et al. 2012).

In a previous work, a systemic functional analysis identified transcription factors (TFs) related to various developmental processes and virulence in *F. graminearum* (Son et al. 2011b). *FgNOT3* (FGSG_13746) was shown to encode the *Sc*Not3 homolog, and Δ*Fgnot3* mutants showed pleiotropic defects in vegetative growth, sexual reproduction, secondary metabolite production, and virulence. We hypothesized that *Fg*Not3 is involved in diverse regulation, leading to severe impacts on numerous features of the fungus. In this present study, we report an in-depth functional analysis of *Fg*Not3, a member of the Ccr4-Not complex, in *F. graminearum*. Furthermore, we demonstrate how the functions of *Fg*Not3 are conserved in this fungus

and elucidate the involvement of the Not module in the developmental stages of *F. graminearum*.

MATERIALS AND METHODS

I. Fungal strains and media

The *F. graminearum* wild-type strain Z-3639 (Bowden and Leslie 1999) and the mutants used in this study are listed in Table 1. For genomic DNA (gDNA) isolation, each strain was inoculated in 5 ml of complete medium (CM) and incubated at 25 °C for 3 days on a rotary shaker at 150 rpm. For fungal sporulation, conidia of all strains were induced on yeast malt agar (YMA) (Harris 2005) and in carboxymethyl cellulose (CMC) medium (Cappellini and Peterson 1965). A rice culture was used to evaluate trichothecene and zearalenone (ZEA) production (Seo et al. 1996). Other media used in this study were prepared and used according to the instructions in the *Fusarium* laboratory manual (Leslie et al. 2006). The wild-type and transgenic strains were stored as mycelia and conidia in 20% glycerol at -80 °C.

Table 1. *F. graminearum* strains used in this study.

Strain	**Genotype**	**Reference, source, or parent strains**
Z-3639	Wild-type	(Bowden and Leslie 1999)
hH1-GFP	*hH1::hH1-GFP-HYG*	(Hong et al. 2010)
mat1g	Δ*mat1-1::GEN hH1::hH1-GFP-HYG*	(Hong et al. 2010)
Δ*Fgnot3*	Δ*Fgnot3::GEN*	(Son et al. 2011b)
FgNot3c	Δ*Fgnot3::FgNOT3-HYG*	This study
Δ*Fgnot3*-g	Δ*Fgnot3::GEN hH1-GFP-HYG*	This study
Δ*Fgnot2*	Δ*Fgnot2::GEN*	This study
FgNot2c	Δ*Fgnot2::FgNOT2-HYG*	This study
Δ*Fgnot4*	Δ*Fgnot4::GEN*	This study
FgNot4c	Δ*Fgnot4::FgNOT4-HYG*	This study

II. Nucleic acid manipulation, primers, and PCR conditions

The gDNA was extracted as previously described (Leslie et al. 2006). Restriction endonuclease digestion, agarose gel electrophoresis, gel blotting, and DNA blot hybridization were performed in accordance with standard techniques (Sambrook and Russell 2001). The polymerase chain reaction (PCR) primers (Table S1) used in this study were synthesized by an oligonucleotide synthesis facility (Bionics, Seoul, Korea).

III. Genetic manipulations and fungal transformations

For complementation of the Δ*Fgnot3* deletion mutants, the wild-type *FgNOT3* allele from *F. graminearum* strain Z-3639 was amplified using the primer pair Not3-5F com/Not3-3N com. The hygromycin resistance cassette (*HYG*) was amplified from the pBCATPH vector using the primer pair pBCATPH/comp 5′For/pBCATPH/comp 3′Rev (Min et al. 2012). The resulting amplicons were fused by double-joint (DJ) PCR as previously described (Yu et al. 2004). The final PCR constructs were obtained by nested PCR and were transformed into the Δ*Fgnot3* deletion mutants as described previously (Han et al. 2007).

To generate *FgNOT2* deletion mutants, the 5′- and 3′-flanking regions of the *FgNOT2* gene and a geneticin resistance cassette (*GEN*) were amplified from Z-3639 and pII99, respectively, and were fused by DJ PCR. The subsequent procedures for the third round of PCR and transformation were the same as for complementation using the *FgNOT3* gene of *F. graminearum*. The *FgNOT4* deletion mutants were produced using the same strategy. The same strategy used for the generation of FgNot3c strains was also applied for the complementation of the Δ*Fgnot2* and Δ*Fgnot4*.

IV. Conidial production and morphology

After each strain was incubated in 50 ml of CM for 72 h at 25 °C on a rotary shaker (150 rpm), mycelia of each strain were harvested and washed twice with distilled water. To induce conidiation, harvested mycelia were spread on YMA and incubated for 48 h at 25 °C under near-UV light (wavelength: 365 nm, HKiv Import & Export Co., Ltd., Xiamen, China). Conidia were collected using distilled water, filtered through cheese cloth, washed, and resuspended in distilled water. After inoculating a 1 ml conidial suspension (1×10^6 conidia/ml) of each strain in 50 ml of CMC and incubating for 5 days at 25 °C on a rotary shaker (150 rpm), the number of conidia produced was counted to measure conidial production with a hemocytometer (Superior,

Marienfeld, Germany). For observation of conidial morphology, the conidia produced by each strain on YMA were harvested, and differential interference contrast (DIC) images were obtained using a DE/Axio Imager A1 microscope (Carl Zeiss, Oberkochen, Germany).

V. Germination assay

To evaluate germination rates, conidial suspensions (1×10^6 conidia/ml) of each strain were inoculated into 20 ml of CM and MM and incubated at 25 °C on a rotary shaker (150 rpm). The germinated conidia per 100 total conidia were counted at 0, 4, 6, 8, 10, 12, 24, 36, 48, and 60 h after inoculation. Conidial germination was defined as the point at which the length of the germ tube is the same as the width of the conidium. The experiments were performed twice with three replicates for each time point.

VI. Outcrosses and virulence test

For self-fertilization, mycelia grown on carrot agar for 5 days were mock-fertilized with 2.5% Tween 60 solution to induce sexual reproduction as previously described (Leslie et al. 2006). For outcrosses, mycelia of the female strain grown on carrot agar plates were fertilized with 1 ml of male strain conidia (1×10^6 conidia/ml).

The heterothallic mat1g (Δ*mat1-1::GEN hH1::hH1-GFP-HYG*) strain (Hong et al. 2010) was used as a tester strain for outcrosses. After sexual induction, the fertilized cultures were incubated for 7 days under near-UV light (HKiv Import & Export Co., Ltd.) at 25 °C.

A virulence test of the fungal strains was performed using the wheat cultivar Eunpamil as previously described (Son et al. 2011a). Briefly, 10 μl of conidial suspensions (1×10^6 conidia/ml) obtained from each strain was point-inoculated into a spikelet of the wheat head at early anthesis. Infected plants were incubated in a humidity chamber for 3 days and subsequently transferred to a green house. After 21 days, the number of spikelets showing disease symptoms was counted.

VII. Quantification of mycotoxins and fungal ergosterol

For trichothecene analysis, the 3-week-old rice cultures were ground and extracted with an ethyl acetate/methanol mixture (4:1, v/v) as previously described (Seo et al. 1996). The extracts were purified using MycoSep® 225 Trich Multifunctional columns (Romer Labs, Inc., Union, MO, USA) and then concentrated to dryness. A portion of each extract was derivatized with Sylon BZT (BSA + TMCS + TMSI, 3:2:3, Supelco, Bellefonte, PA, USA) and analyzed using a Shimadzu QP-5000 gas chromatograph-mass spectrometer (GC-MS; Shimadzu,

Kyoto, Japan). ZEA was extracted from rice cultures using the same strategy and analyzed using an HPLC system with a RF-10A XL fluorescence detector (Shimadzu) (Seo et al. 1996). To quantify fungal ergosterol, ground rice cultures (1 g) were extracted in 4 ml of chloroform/methanol (2:1, v/v) as previously described (Kim et al. 2011). Ergosterol was analyzed using a HPLC system with a 4.6 U ODS column (250×4.6 mm, Phenomenex, Madrid Avenue Torrance, CA, USA) and a UV detector (Shimadzu) set to measure absorbance at 282 nm. Quantities were determined by comparing peak areas of samples to those of a standard curve generated from HPLC-grade ergosterol (Sigma-Aldrich, St. Louis, Missouri, USA). The experiments were repeated three times.

VIII. Quantitative real-time (qRT)-PCR

Total RNA of the wild-type and Δ*Fgnot3* strains was extracted from mycelia at 18 h after inoculation in CMC using an Easy-Spin total RNA extraction kit (Intron Biotech, Seongnam, Korea) (Jonkers et al. 2012). First-strand cDNA was synthesized with the SuperScript III First-Strand Synthesis System (Invitrogen, Carlsbad, CA, USA) using oligo$(dT)_{20}$ according to the manufacturer's recommendations. qRT-PCR was performed using iQ SYBR Green Master Mix (Bio-Rad, Hercules, CA, USA) and a 7500 real-time PCR system (Applied

Biosystems, Foster City, CA, USA). The endogenous housekeeping gene ubiquitin C-terminal hydrolase (*UBH*; FGSG_01231) was used for normalization (Kim and Yun 2011). The PCR assays were repeated three times with two biological replicates. The threshold cycle (ΔC_T) value of gene expression was subtracted from the ΔC_T value of each sample to obtain a $\Delta\Delta C_T$ value. The transcript level relative to the calibrator was expressed as $2^{-\Delta\Delta CT}$ (Livak and Schmittgen 2001).

IX. Yeast strains and complementation assay

The *S. cerevisiae* strains BY4741 (wild-type) and YPR072w (Δ*Scnot5*) were obtained from EUROSCARF (http://web.uni-frankfurt.de/fb15/mikro/euroscarf/) and maintained on yeast extract peptone dextrose (YPD) medium. The *FgNOT3* ORF was amplified from first-strand cDNA of the *F. graminearum* wild-type strain Z-3639 with the primer pair Not3-cloning-F/Not3-cloning-R (Table S1) by PCR, digested by restriction enzymes BstXI and XbaI, and subsequently cloned into the BstXI and XbaI sites of pYES2 (Invitrogen). The pYES2-*FgNOT3* construct was introduced into the Δ*Scnot5* strain using the lithium acetate method (Gietz and Schiestl 2007) after verification of the construct by sequencing (Macrogen Inc., Seoul, Korea). In addition, the empty vector pYES2 was simultaneously introduced into yeast wild-type BY4741 and Δ*Scnot5*.

Synthetic complete medium lacking uracil (SC-Ura) and supplemented with ampicillin (0.2 mg/ml) was used for the selection and isolation of transformants (Gietz and Schiestl 2007). For the complementation assay, yeast cells were cultured for 3 days at 30 °C on a rotary shaker (200 rpm) in SC-Ura supplemented with ampicillin, harvested, and then diluted in distilled water. Aliquots of 10 µl were point-inoculated on SC-Ura supplemented with ampicillin followed by incubation for 4 days at 30 °C.

RESULTS

I. Molecular characterization of the *FgNOT3* gene

The Ccr4-Not complex of *S. cerevisiae* consists of two major modules, the catalytic module (*Sc*Caf1 and *Sc*Ccr4) and the Not module (*Sc*Not1, *Sc*Not2, *Sc*Not3, *Sc*Not4, and *Sc*Not5), and additional two subunits, *Sc*Caf40 and *Sc*Caf130 (Bai et al. 1999; Maillet et al. 2000). The occurrence of the subunit genes in the Ccr4-Not complex in representative species based on the STRING database (Szklarczyk et al. 2011) showed that most of these genes are highly conserved in eukaryotes (Fig. 1A). However, Caf130 homologs are specifically conserved in members of the Saccharomycetaceae, such as *S. cerevisiae* and *Candida glabrata*.

Except for fungal species of the Saccharomycetaceae, only single gene encoding proteins similar to *Sc*Not3 or *Sc*Not5 have been identified in other eukaryotic genomes (Fig. 1A). Although Not3/5 of oomycetes, *Phytophthora infestans* and *Pythium ultimum* showed higher sequence identity with *Sc*Not5 than *Sc*Not3, the rest of the single proteins were homologs for *Sc*Not3. Previous reports have also shown that Not5 is not conserved in animals and is specific for the Saccharomycetaceae (Panepinto et al. 2013). Phylogenetic analyses of Not3 homologs showed that Not3 homologs in filamentous fungi were clustered into a separate group relative to yeasts and animals (Fig. 1B).

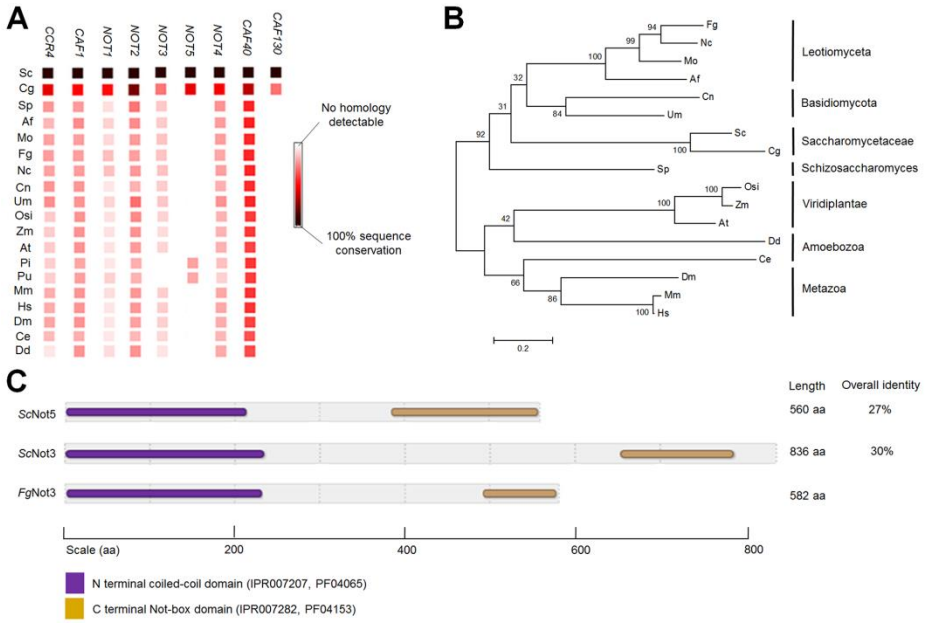

Figure 1. Molecular characterization of *Fg*Not3. (**A**) Occurrences of subunit genes of the Ccr4-Not complex homologs in representative species. The occurrence image was constructed using the STRING database (Szklarczyk et al. 2011). Sc, *Saccharomyces cerevisiae*; Cg, *Candida glabrata*; Sp, *Schizosaccharomyces pombe*; Af, *Aspergillus fumigatus*; Mo, *Magnaporthe oryzae*; Fg, *Fusarium graminearum*; Nc, *Neurospora crassa*; Cn, *Cryptococcus neoformans*; Um, *Ustilago maydis*; Osi, *Oryza sativa Indica*; Zm, *Zea mays*; At, *Arabidopsis thaliana*; Pi, *Phytophthora infestans*; Pu, *Pythium ultimum*; Mm, *Mus musculus*; Hs, *Homo sapiens*; Dm, *Drosophila melanogaster*; Ce, *Caenorhabditis elegans*; Dd, *Dictyostelium discoideum*. (**B**) Phylogenetic tree of homologs of the Not3 subunit from the Ccr4-Not complex from representative species constructed using amino acid

sequences comparison. (**C**) Schematic presentation of the conserved regions of Not3 subunit homologs between *S. cerevisiae* and *F. graminearum*. The percentage of identity between two proteins was calculated using the ALIGN algorithm (global alignment with no short-cuts). Different shadings denote the domain entries in the InterPro database (http://www.ebi.ac.uk/interpro/) and the HMMPham database (http://pfam.sanger.ac.uk/).

BLASTp searches for both *Sc*Not3 and *Sc*Not5 in the *F. graminearum* genome (http://www.broadinstitute.org) identified the FGSG_13746 locus encoding 582 amino acids (30% and 27% overall identity to *Sc*Not3 and *Sc*Not5, respectively). The protein harbored two significant domains (IPR007207 and IPR007282) similar to those of both *Sc*Not3 and *Sc*Not5 (Fig. 1C). Further analysis of the conserved protein sequences of partial N-terminal regions showed that FGSG_13746 shares 55% and 50% identity with those of *Sc*Not3 and *Sc*Not5, respectively. The human C-terminal region of Not3 also shows 24% overall identity to both *Sc*Not3 and *Sc*Not5, although their N-terminal regions share 41% and 39% identity with those of *Sc*Not3 and *Sc*Not5, respectively (Albert et al. 2000). Based on these combined results, we designated the protein encoded by FGSG_13746 as *Fg*Not3.

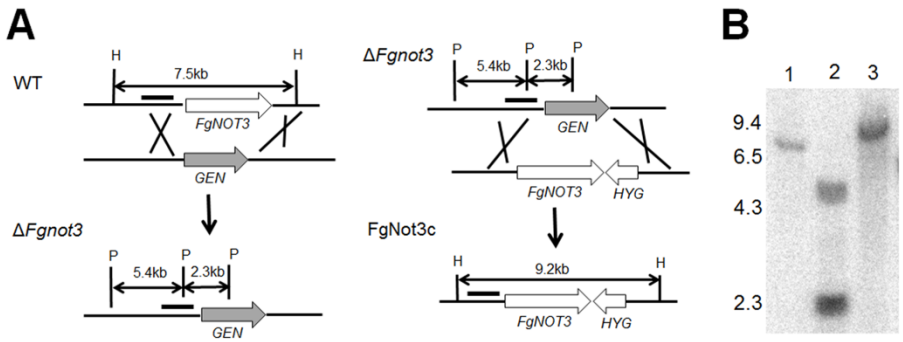

Figure 2. Targeted deletion and complementation of Δ*Fgnot3*. (**A**) Strategies used for the deletion and complementation of Δ*Fgnot3*. The 5′-flanking regions (black bars) of the *FgNOT3* ORF were used as probes for hybridization. WT, wild-type strain Z-3639; Δ*Fgnot3*, *FgNOT3* deletion mutant; FgNot3c, Δ*Fgnot3*-derived strain complemented with *FgNOT3*; H, HindIII; P, PstI; *GEN*, geneticin resistance gene cassette; *HYG*, hygromycin B resistance gene cassette. (**B**) Southern blot analysis of the deletion and complementation of Δ*Fgnot3*. Lane 1, wild-type strain Z-3639; lane 2, deletion mutant; lane 3, complementation strain. The sizes of DNA standards (kb) are indicated to the left of the blot.

II. Effects of *FgNOT3* deletion on vegetative growth, conidiogenesis, and germination

The *FgNOT3* deletion mutants were obtained from a mutant library of *F. graminearum* TF deletions (Son et al. 2011b). For genetic complementation, the construct containing the *FgNOT3* open reading frame (ORF) fused with *HYG* was introduced into the protoplast of the Δ*Fgnot3* strain (Fig. 2). Southern blot analysis showed that the construct successfully replaced *GEN* in the genome of the complementation strain, resulting in FgNot3c strains. The Δ*Fgnot3* strains showed markedly reduced radial growth (~50%) and aerial mycelia on both complete medium (CM) and minimal medium (MM) (Fig. 3A).

To further determine features affecting defective growth of the Δ*Fgnot3* mutants, we performed microscopic observation. Deletion of *FgNOT3* resulted in a hyper-branching phenotype compared to the wild-type strain (Fig. 3B). Furthermore, the hyphae of Δ*Fgnot3* mutants tended to be abnormally swollen, with the swollen hyphae resulting in distorted branching (Fig. 3C). These results demonstrated that *FgNOT3* is required for normal growth and mycelial morphology in *F. graminearum*.

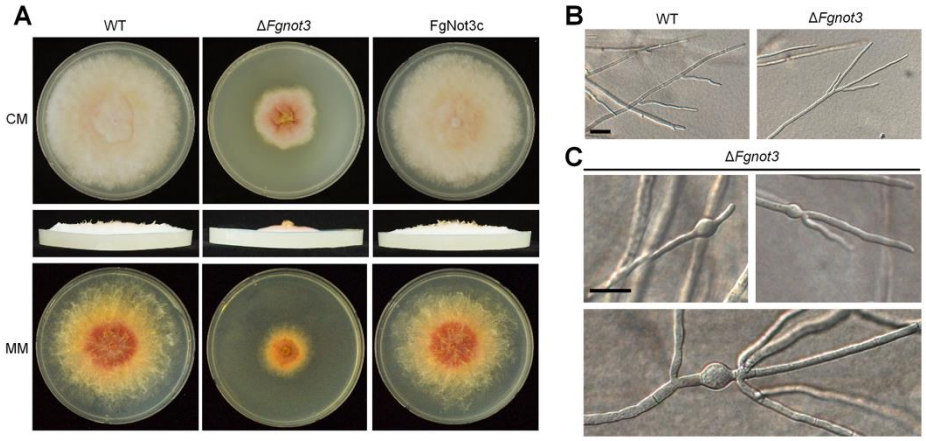

Figure 3. The vegetative growth of Δ*Fgnot3* mutants. (**A**) Mycelial growth on complete medium (CM) and minimal medium (MM). The pictures were taken 5 days after inoculation. The pictures were taken from the upper (top) and the side (middle) of the plates. (**B**) Microscopic observation of hyphae. The differential interference contrast (DIC) images were taken 2 days after inoculation. Scale bar = 50 μm. (**C**) Swollen hyphae of Δ*Fgnot3* mutants on CM agar. Scale bar = 50 μm. WT, *F. graminearum* wild-type strain Z-3639; Δ*Fgnot3*, *FgNOT3* deletion mutant; FgNot3c, Δ*Fgnot3*-derived strain complemented with *FgNOT3*.

Deletion of *FgNOT3* also resulted in severe defects in asexual sporulation. The conidial production of the Δ*Fgnot3* strain in CMC medium was significantly reduced compared to the wild-type and complemented strains (Fig. 4A). Moreover, conidia of Δ*Fgnot3* strains were abnormally shaped (Fig. 4B). The conidia of the Δ*Fgnot3* strains were shorter and wider than the wild-type (Table 2 and Fig. 4B). Deletion of *FgNOT3* also resulted in a reduced septum number.

To determine how deletion of *FgNOT3* affects conidiogenesis in *F. graminearum*, we generated the Δ*Fgnot3*-g strains (Δ*Fgnot3::GEN hH1-GFP-HYG*) by an outcross between the mat1g (Hong et al. 2010) and Δ*Fgnot3* strains. Dozens of ascospores were isolated, and their genotypes were confirmed by fluorescence microscopy and PCR. The hH1-GFP strain carrying the wild-type allele of *FgNOT3* initially produced phialides from the hyphae, and mature phialide cells continuously produced conidia (Fig. 4C). Additionally, conidia were often directly produced from the hyphae. In contrast, deletion of the *FgNOT3* mostly abolished phialide production, and most conidia were directly produced from the hyphae (Fig. 4C). All of these defects were restored to wild type levels in the FgNot3c complemented strains.

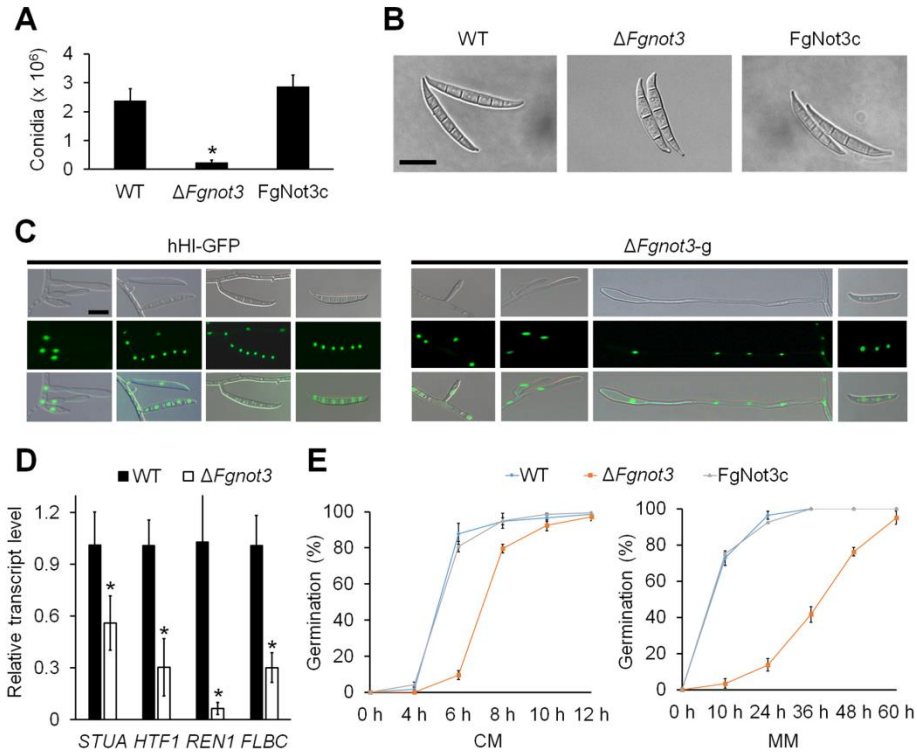

Figure 4. Conidiation and germination of Δ*Fgnot3* mutants. (**A**) Conidial production. The number of conidia was counted after 5 days of incubation in CMC. The values were generated based on three biological replicates. Significant differences ($P < 0.05$) are indicated with an asterisk. (**B**) Conidial morphology. Conidia were induced on YMA and subsequently observed by DIC. Scale bar = 20 μm. (**C**) Morphology of conidiophores in *F. graminearum* strains. Pictures were taken 1 to 3 days after conidium induction. Scale bar = 10 μm. (**D**) Relative transcript levels of genes related to conidiation. Total RNA of the wild-type and Δ*Fgnot3* strains was extracted 18 h after inoculation in CMC. The relative transcript levels of each subunit gene in wild type were arbitrarily set to 1. Significant differences ($P < 0.05$) are indicated

with an asterisk. (**E**) Germination rate. The percentage of conidium germination in CM and MM. WT, *F. graminearum* wild-type strain Z-3639; Δ*Fgnot3*, *FgNOT3* deletion mutant; FgNot3c, Δ*Fgnot3*-derived strain complemented with *FgNOT3*.

Table 2. Conidial morphology and virulence of Δ*Fgnot3* mutants.

Strain	Conidial morphology[a]			Virulence
	Length (μm)	Width (μm)	No. of septa	(disease index)[c]
Z-3639	46.8±1.8A[b]	6.1±0.1A	4.0±0.1A	9.7±4.1A
Δ*Fgnot3*	41.2±0.2B	7.1±0.4B	3.4±0.1B	0.45±0.3B
FgNot3c	45.3±1.3A	6.2±0.1A	4.0±0.1A	9.6±2.6A

[a] Conidia were harvested from a 1-day-old YMA culture.

[b] The presented data are average values ± standard deviations. Values within a column with different letters are significantly different ($P < 0.05$) based on Tukey's HSD test.

[c] The disease index (number of diseased spikelets per wheat head) of the strains was measured 21 days after inoculation.

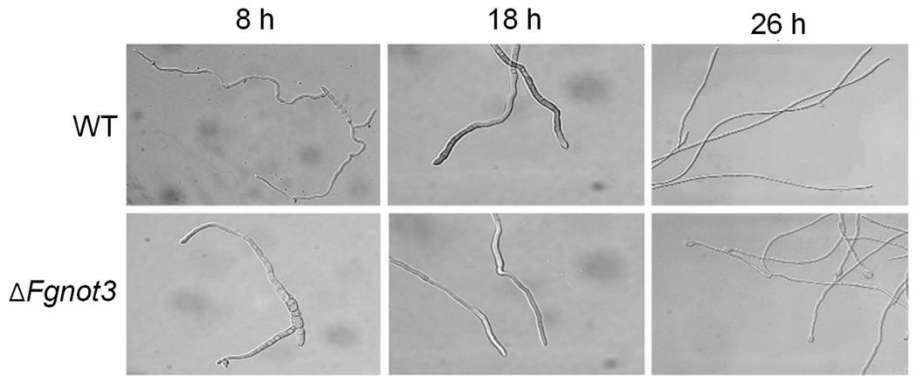

Figure 5. The mycelial morphology of Δ*Fgnot3* mutants on CM liquid medium. The mycelial morphology was observed on CM liquid medium after incubating for 8 h, 18 h, and 26 h. WT, wild-type strain Z-3639; Δ*Fgnot3*, *FgNOT3* deletion mutant; FgNot3c, Δ*Fgnot3*-derived strain complemented with *FgNOT3*.

To test the hypothesis that *Fg*Not3 plays a role in regulating expression of genes related to conidiogenesis, we compared the transcript levels of representative conidiation-related genes in the wild-type and Δ*Fgnot3* deletion mutant strains (Ohara et al. 2004; Lysoe et al. 2011; Son et al. 2011b; Zheng et al. 2012). Transcript levels of four genes, *STUA*, *HTF1*, *REN1*, and *FLBC*, were significantly decreased in the Δ*Fgnot3* mutants compared to wild type (Fig. 4D). Interestingly, transcript levels of *ABAA* and *WETA*, the transcription factors specifically involved in conidiogenesis in *F. graminearum* (Son et al. 2013; Son et al. 2014), were not altered when *FgNOT3* was deleted (data not shown).

The conidia germination rates of Δ*Fgnot3* mutants were greatly reduced in both CM and MM compared to wild type (Fig. 4E). Approximately 90% of conidia in the wild-type strain germinated 6 h after inoculation in CM, whereas only ~10% of conidia germinated in the Δ*Fgnot3* mutants (Fig. 4E). Furthermore, only ~16% of Δ*Fgnot3* mutant conidia germinated in MM 24 h after inoculation, whereas most wild type conidia were germinated after 24 h. Although the germinated hyphae of all strains showed an identical morphology up to 24 h after inoculation in CM (Fig. 5), the germinated hyphae of Δ*Fgnot3* mutants exhibited swollen tips 26 h after inoculation (Fig. 5 and 3C). All defects of the Δ*Fgnot3* mutants were restored in the FgNot3c complemented

strains.

III. *FgNOT3* is important for sexual development and virulence

The fertility of the *F. graminearum* strains was determined on carrot agar. In self-fertility, the wild-type strains began to produce detectable perithecial initials 3 days after sexual induction, and mature perithecia were produced after an additional 3 or 4 days of incubation (Fig. 6A). In contrast to wild type, the Δ*Fgnot3* mutants only produced a few perithecium initials that did not mature.

Subsequently, we determined the female and male fertilities of the Δ*Fgnot3* mutants based on outcross analyses. When the Δ*Fgnot3* mutant was spermatized with wild-type or Δ*mat1* strains, no mature perithecium was produced, similar to the self-cross of the Δ*Fgnot3* mutants (Fig. 6A). However, when the Δ*Fgnot3* mutant was used as a male in the outcross of Δ*mat1* (female) × Δ*Fgnot3* (male), normal perithecia were produced, and the progeny with or without the hH1-Gfp signal were segregated 1:1 in accordance with Mendelian genetics, suggesting that *FgNOT3* is not necessary for male fertility (Fig. 6B). The sexual defects of the Δ*Fgnot3* mutants were recovered in the FgNot3c strains.

To evaluate the pathogenicity of the Δ*Fgnot3* mutants in

flowering wheat heads, conidial suspensions of each strain were point-inoculated on spikelets. The results showed that wild-type and FgNot3c strains caused typical head blight symptoms 21 days after inoculation, whereas the Δ*Fgnot3* strains were unable to spread from the inoculated spikelet to adjacent spikelets on the heads (Table 2 and Fig. 6C).

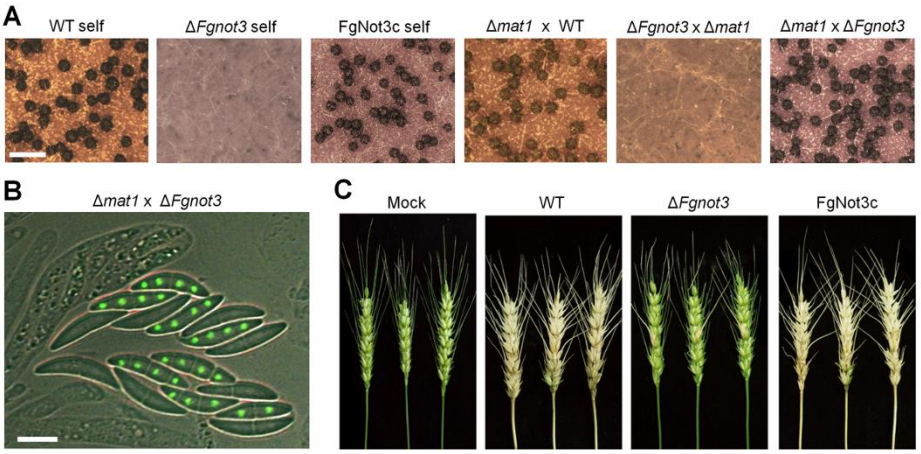

Figure 6. The sexual development and virulence of Δ*Fgnot3* mutants. (**A**) Fertility tests. Each strain was inoculated on carrot agar and mock-fertilized (self-cross) or outcrossed with the corresponding male strain (WT, Δ*Fgnot3* and Δ*mat1*) outcrosses, respectively. The photographs were taken 7 days after sexual induction. Scale bar = 500 μm. (**B**) Asci of an outcross Δ*mat1* × Δ*Fgnot3*. Eight ascospores of an ascus from the Δ*mat1* × Δ*Fgnot3* outcross showing 1:1 segregation with and without Gfp-tagged histone H1. The photographs were taken 9 days after sexual induction. Scale bar = 10 μm. (**C**) Virulence on wheat heads. The center spikelet of each wheat head was injected with 10 μl of a conidial suspension. Pictures were taken 21 days after inoculation. Mock, negative control mock-inoculated with 0.01% of Tween 20; WT, *F. graminearum* wild-type strain Z-3639; Δ*Fgnot3*, *FgNOT3* deletion mutant; FgNot3c, Δ*Fgnot3*-derived strain complemented with *FgNOT3*.

IV. *FgNOT3* is required for normal growth under high-temperature conditions

To characterize the roles of *FgNOT3* in environmental stress responses, we examined the sensitivity of the Δ*Fgnot3* mutants to various stresses, including carbon and nitrogen starvation, osmotic and oxidative stresses, cell wall-damaging agents, fungicide exposure, and thermal stresses. There were no specific stresses or agents that affected the growth of Δ*Fgnot3* mutants, as previously described (data not shown). However, we identified the role of *FgNOT3* in adaptation to thermal stress in *F. graminearum*. The Δ*Fgnot3* mutants exhibited increased sensitivity to high temperature and could not grow at 31 °C (Fig. 7).

V. *Fg*Not3 functions together with other Not subunits of the Ccr4-Not complex

The effects of *FgNOT3* deletion on the transcript levels of nine putative Ccr4-Not complex subunit genes were analyzed during conidiation (Fig. 8). Five genes (homologs for *CCR4*, *CAF1*, *CAF40*, *CAF130*, and *DDH1*) showed similar transcript levels between the wild-type and Δ*Fgnot3* strains. However, transcript levels of *FgNOT1* and *FgNOT4* in the Δ*Fgnot3* mutants were significantly decreased

compared to the wild-type (Fig. 8). *FgNOT2* transcript level of the Δ*Fgnot3* mutants were highly increased, showing more than 6-fold greater expression compared to wild type (Fig. 8).

Because *FgNOT1* is an essential gene (Son et al. 2011b) and Δ*Fgnot3* showed pleiotropic defects, we sought to determine how other Not subunits affect the developmental stages of *F. graminearum*. To characterize their biological functions, we generated deletion and complementation mutants of *FgNOT2* (FGSG_12685) and *FgNOT4* (FGSG_09233) via homologous recombination (Fig. 9). We found that the radial growth, conidial production and morphology, sexual development, and virulence of both Δ*Fgnot2* and Δ*Fgnot4* mutants were severely impaired compared to the wild-type, similar to the observed phenotypes of the Δ*Fgnot3* strains (Fig. 10 and 11, and Table 3). In particular, deletion of *FgNOT2* and *FgNOT4* resulted in markedly reduced radial growth compared to the wild-type and complemented strains (Fig. 10). Furthermore, Δ*Fgnot2* and Δ*Fgnot4* mutants also exhibited increased sensitivity to high temperature (Fig. 7).

Conidial production of both the Δ*Fgnot2* and Δ*Fgnot4* mutants was similarly reduced compared to wild type (Table 3). Deletion of *FgNOT2* resulted in more severe defects in conidial morphologies than *FgNOT4* deletion (Table 3 and Fig. 11A). Whereas the Δ*Fgnot3* mutants showed an almost complete lack of phialide formation, the

Δ*Fgnot2* and Δ*Fgnot4* mutants mainly produced normal phialides and conidia (Fig. 11B). Approximately 30% of the phialides of both Δ*Fgnot2* and Δ*Fgnot4* mutants were produced as cluster forms with abnormal shapes.

We found that deletion of *FgNOT2* and *FgNOT4* also resulted in a loss of self and female fertilities (Fig. 11C,D) and a significant decrease in virulence on wheat heads (Table 3 and Fig. 11E). All of these defects of the Δ*Fgnot2* and Δ*Fgnot4* mutants were restored to wide type levels in the corresponding complemented strains.

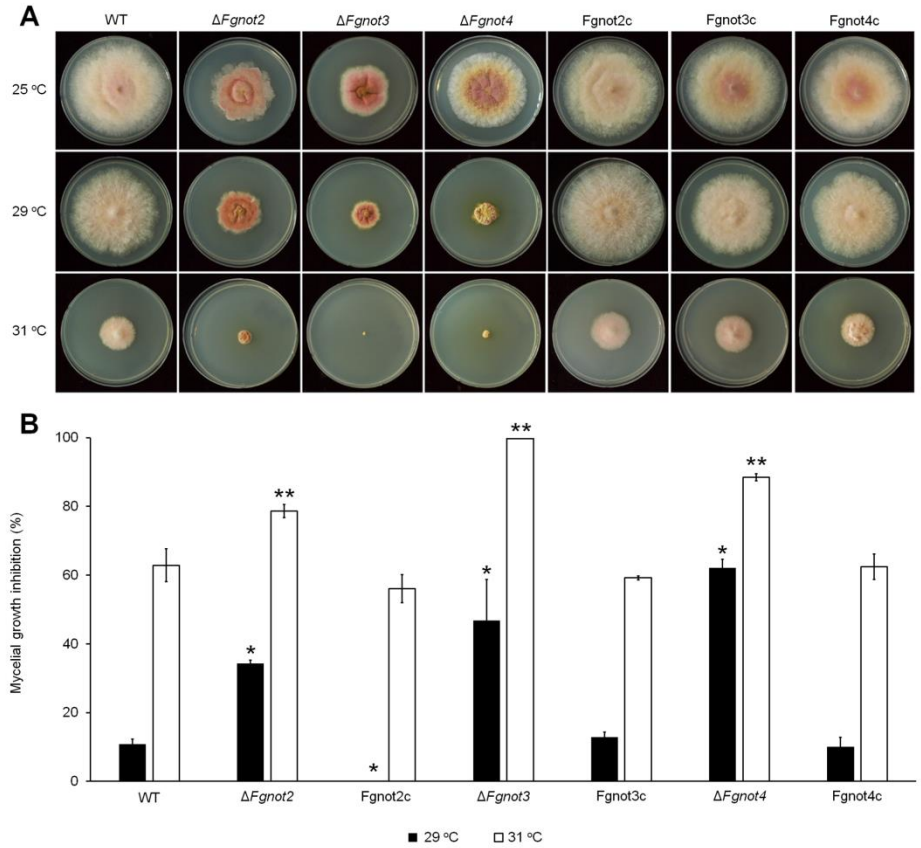

Figure 7. Sensitivity to thermal stress. (**A**) Mycelial growth at different temperatures. (**B**) Each strain was inoculated on CM and incubated at 25 °C, 29 °C, and 31 °C for 5 days. The percentage of the mycelial radial growth inhibition was calculated using the following equation: [(C–N)/C] × 100, where, C is colony diameter of the control (at 25 ^{o}C), and N is that of treatments (at 29 °C and 31 °C) as previously described (Jiang et al. 2011). The values were generated based on three biological replicates. The significance of differences between the wild-type and each strain was calculated using Student's T-test; significant differences ($P < 0.05$) are indicated with an asterisk for 29 °C condition or a double asterisk for 31 ^{o}C condition. WT, *F.*

graminearum wild-type strain Z-3639; Δ*Fgnot3*, *FgNOT3* deletion mutant; FgNot3c, Δ*Fgnot3*-derived strain complemented with *FgNOT3*.

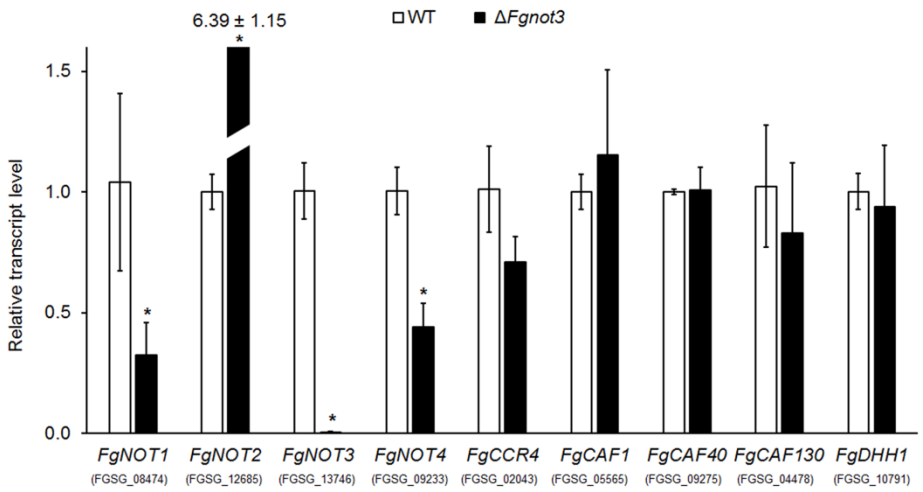

Figure 8. Relative transcript levels of subunits of the Ccr4-Not complex during the conidium induction stage. Total RNA of the wild-type and Δ*Fgnot3* strains was extracted 18 h after inoculation in CMC. The relative transcript levels of each subunit in the Ccr4-Not complex in wild type were arbitrarily set to 1. Significant differences ($P < 0.05$) are indicated with an asterisk.

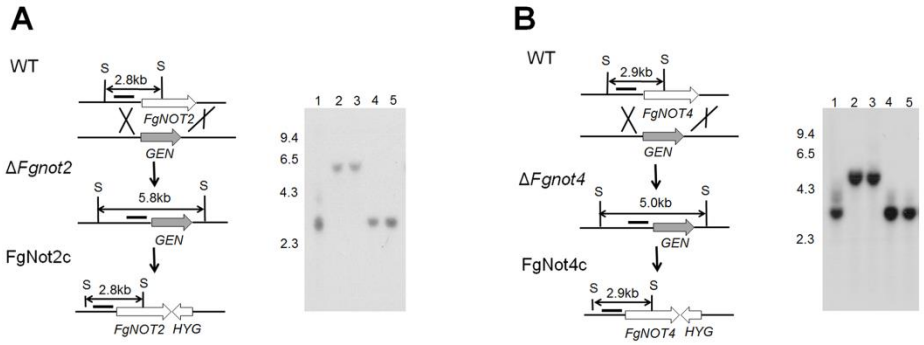

Figure 9. Targeted deletion and mutant complementation strategies for *FgNOT2* (A) and *FgNOT4* (B). The 5′-flanking regions (black bars) of *FgNOT2* ORF and *FgNOT4* ORF were used as probes for hybridization. WT, wild-type strain Z-3639; Δ*Fgnot2*, *FgNOT2* deletion mutant; FgNot2c, Δ*Fgnot2*-derived strain complemented with *FgNOT2*; Δ*Fgnot4*, *FgNOT4* deletion mutant; FgNot4c, Δ*Fgnot4*-derived strain complemented with *FgNOT4*; S, SacI; *GEN*, geneticin resistance gene cassette. Lane 1, wild-type strain Z-3639; lanes 2 and 3, deletion mutants; lanes 4 and 5, complementation strains. The sizes of DNA standards (kb) are indicated to the left of the blot.

Table 3. Vegetative growth, conidial production and morphology, and virulence of Δ*Fgnot2* and Δ*Fgnot4* mutants.

Strain	Radial growth (mm)[a]	Conidial production (10^6/ml)[b]	Conidial morphology[c]			Virulence
			Length (µm)	Width (µm)	No. of septa	(disease index)[d]
Z-3639	64.4±1.1A[e]	3.1±0.5A	45.5±0.9A	5.8±0.2A	4.0±0.1A	9.8±2.3A
Δ*Fgnot2*	50.2±1.2B	2.0±0.2B	42.9±0.2B	7.2±0.2B	3.3±0.1B	0.8±0.3B
FgNot2c	65.2±1.0A	2.9±0.2A	43.6±0.4B	6.1±0.1AC	4.0±0.1A	8.6±4.6A
Δ*Fgnot4*	45.0±1.1C	2.2±0.3B	43.2±0.4B	5.9±0.1A	4.0±0.1A	2.8±2.1B
FgNot4c	65.6±1.6A	3.2±0.3A	46.4±1.0C	6.3±0.2C	4.2±0.2A	9.0±4.4A

[a] Radial growth was measured 4 days after inoculation on CM plates.

[b] Conidia were counted 5 days after inoculation in CMC.

[c] Conidia were harvested from a 1-day-old YMA culture.

[d] The disease index (number of diseased spikelets per wheat head) of the strains was measured 21 days after inoculation.

[e] The presented data are average values ± standard deviations. Values within a column with different letters are significantly different ($P < 0.05$) based on Tukey's HSD test.

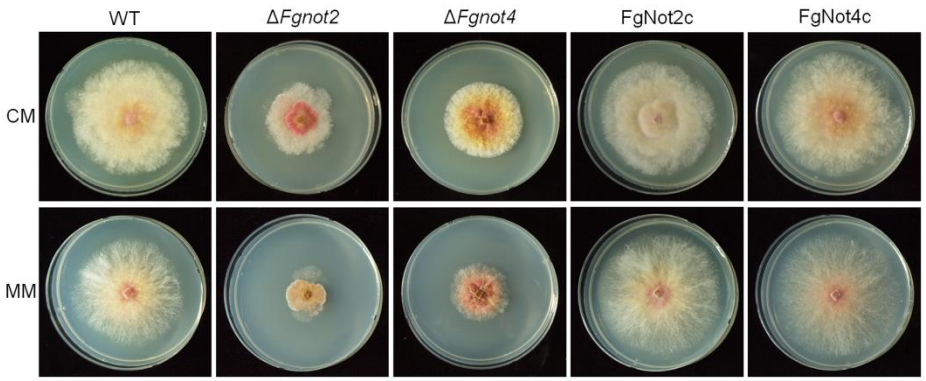

Figure 10. The vegetative growth of Δ*Fgnot2* and Δ*Fgnot4* mutants. Pictures were taken 4 days after inoculation on CM and MM. WT, wild-type strain Z-3639; Δ*Fgnot2*, *FgNOT2* deletion mutant; FgNot2c, Δ*Fgnot2*-derived strain complemented with *FgNOT2*; Δ*Fgnot4*, *FgNOT4* deletion mutant; FgNot4c, Δ*Fgnot4*-derived strain complemented with *FgNOT4*.

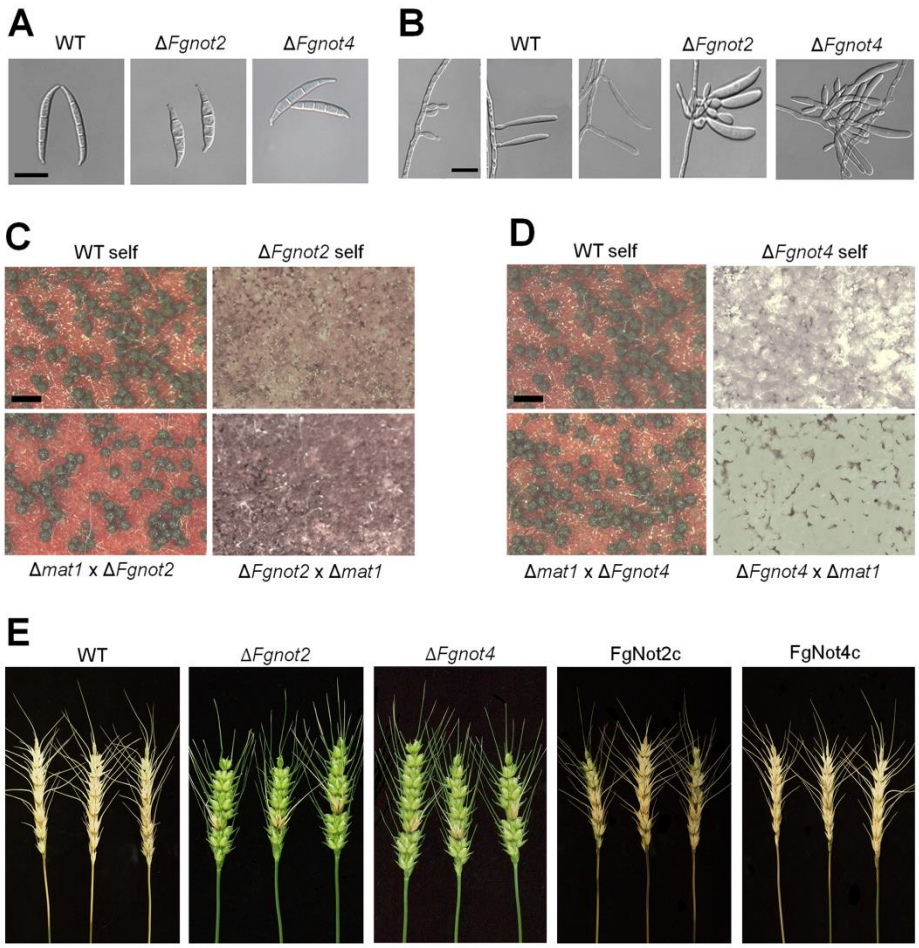

Figure 11. Phenotypes of Δ*Fgnot2* and Δ*Fgnot4* mutants. (**A**) Conidial morphology. Conidia were induced on YMA and subsequently observed by DIC. Scale bar = 20 µm. (**B**) Morphologies of conidiophores. Scale bar = 20 µm. (**C-D**) Fertility tests of Δ*Fgnot2* (**C**) and Δ*Fgnot4* (**D**). Each strain was inoculated on carrot agar and mock fertilized (self-cross) or outcrossed with a respective male strain (WT, Δ*Fgnot2*, Δ*Fgnot4,* and Δ*mat1*). Pictures were taken 7 days after sexual induction. Scale bar = 500 µm. (**E**) Virulence on wheat heads. The center spikelet of each wheat head was injected with 10 µl of a conidial suspension. Pictures were taken 21 days after inoculation. WT, wild-

type strain Z-3639; Δ*Fgnot2*, *FgNOT2* deletion mutant; FgNot2c, Δ*Fgnot2*-derived strain complemented with *FgNOT2*; Δ*Fgnot4*, *FgNOT4* deletion mutant; FgNot4c, Δ*Fgnot4*-derived strain complemented with *FgNOT4*.

VI. *FgNOT2*, *FgNOT3*, and *FgNOT4* are all involved in secondary metabolite production

Whereas Δ*Fgnot4* mutants only produced significantly higher levels of ZEA than the wild-type strain, deletion of both *FgNOT2* and *FgNOT3* resulted in much higher production of both trichothecenes and ZEA in rice cultures (Fig. 12). These observed defects in the Δ*Fgnot2*, Δ*Fgnot3,* and Δ*Fgnot4* mutants were restored in the corresponding complemented strains.

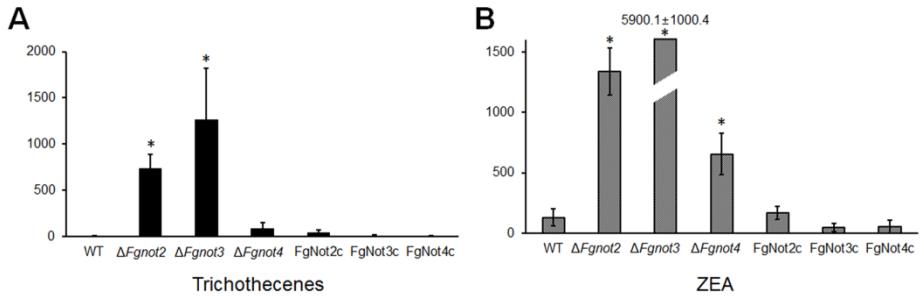

Figure 12. Mycotoxin production of Δ*Fgnot2*, Δ*Fgnot3,* and Δ*Fgnot4* mutants. Total trichothecenes and zearalenone (ZEA) production was normalized to fungal ergosterol levels with the following equation: [trichothecenes or ZEA production (μg/g)/ergosterol contents (μg/g)] × 100, as previously described (Kim et al. 2011). The values were generated based on three biological replicates. The significance of differences between the wild-type and each strain was calculated using Student's T-test; significant differences ($P < 0.05$) are indicated with an asterisk. WT, wild-type strain Z-3639; Δ*Fgnot2*, *FgNOT2* deletion mutant; FgNot2c, Δ*Fgnot2*-derived strain complemented with *FgNOT2*; Δ*Fgnot3*, *FgNOT3* deletion mutant; FgNot3c, Δ*Fgnot3*-derived strain complemented with *FgNOT3*; Δ*Fgnot4*, *FgNOT4* deletion mutant; FgNot4c, Δ*Fgnot4*-derived strain complemented with *FgNOT4*.

DISCUSSION

In this study, *FgNOT3* was found to be involved in numerous developmental stages in *F. graminearum*, including vegetative growth, asexual and sexual reproduction, secondary metabolite production, and virulence. Moreover, we provided genetic evidence that other Not subunits also have conserved roles in this fungus. Taken together, these results demonstrate that the Not module of the Ccr4-Not complex plays critical roles in the regulation of multiple and complex cellular processes and differentiation in *F. graminearum*.

*Fg*Not3 contributes to hyphal morphogenesis and virulence in *F. graminearum*. Deletion of *FgNOT3* led to a significant reduction in mycelial production and abnormal-shaped hyphae in *F. graminearum,* phenotypes similar to other model eukaryotes. Yeast *ScNOT5* is involved in diverse processes, including cell wall integrity and filamentation (Oberholzer and Collart 1998; Collart 2003). Deletion of *CaNOT5* also resulted in defective morphogenesis and virulence in *Candida albicans* (Cheng et al. 2005). Although the Δ*Fgnot3* mutants produced a considerable amount of trichothecenes, a virulence factor (Proctor et al. 1995), virulence of the mutants was completely abolished, and fungal growth was restricted to infection sites. We believe that the Δ*Fgnot3* mutant hyphae could not differentiate into structures required for host infection due to the attenuated

morphogenesis and cellular differentiation. It has been reported that *F. graminearum* hyphae develop mats and appressoria-like structures to penetrate the host cell wall (Jansen et al. 2005; Boenisch and Schäfer 2011).

*Fg*Not3 also regulates hyphal differentiation required for both sexual and asexual reproduction in *F. graminearum*. Both ascospores and conidia are produced from highly differentiated hyphal structures such as perithecia and phialides, respectively. Δ*Fgnot3* mutants completely lost female fertility and failed to produce normal phialide cells, leading to markedly impaired spore production and abnormal conidium morphologies. The significant down-regulation of genes involved in conidiation, including *STUA*, *HTF1*, *REN1*, and *FLBC,* but not *ABAA* and *WETA*, supports the hypothesis that *FgNOT3* has global roles in asexual sporulation independent of the AbaA-WetA pathway. To our knowledge, this is the first report to implicate the contribution of Not3 homologs in both sexual and asexual developmental stages.

NOT3/5 mutations in yeasts affect cell wall structure, and therefore, the null mutants showed altered sensitivities to cell wall stress-inducing agents. Although Δ*Canot5* mutants of *C. albicans* were highly sensitive to Calcofluor white, they were more resistant to β-glucanase zymolyase than wild type (Cheng et al. 2005). Δ*Scnot3* mutants showed increased sensitivity to caffeine in *S. cerevisiae*

(Kapitzky et al. 2010). However, *FgNOT3* deletion mutants did not show any altered sensitivity to cell wall stress-inducing agents as well as other specific stresses as previously reported (data not shown) (Son et al. 2011b). Intriguingly, we identified a novel function of *FgNOT3* in adaptation to thermal stress. Moreover, *FgNOT3* did not complement the *S. cerevisiae* Δ*Scnot5* mutant (Fig. S1). Differences in the function of Not3/5 in cell wall integrity between yeast and filamentous fungi may not only be derived from evolutionary divergence between the two groups but also might explain the diverse roles of Not3/5 in cellular processes among eukaryotes. *C*Not3 in mice is essential for multiple functions, including embryonic development and control of heart function, and the metabolism of adult mice supports this notion (Neely et al. 2010; Morita et al. 2011).

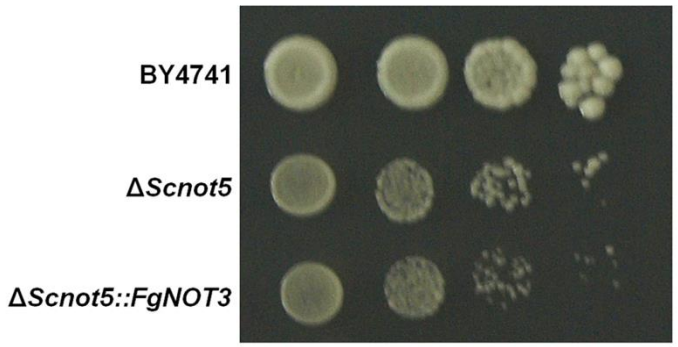

Figure S1. Complementation assay of *FgNOT3* on *S. cerevisiae* Δ*Scnot5*. Cells were cultured for 3 days at 30 °C at 200 rpm in SC lacking Ura (SC-Ura) supplemented with ampicillin medium, harvested, and then diluted in distilled water. Aliquots of 10 µl were point-inoculated on SC-Ura supplemented with ampicillin medium and incubated for 4 days at 30 °C. Columns in each panel represent serial log dilutions. BY4741, *S. cerevisiae* wild-type strains BY4741 harboring plasmid pYES2; Δ*Scnot5*, *S. cerevisiae* deletion of *Scnot5* mutant harboring plasmid pYES2; Δ*Scnot5::FgNOT3*, *S. cerevisiae* Δ*Scnot5*-derived strain complemented with *F. graminearum FgNOT3*.

Our transcript analyses provide some clues for understanding the interactions among the subunits of Ccr4-Not complex. Transcript levels of all Not subunits, including *FgNOT1*, *FgNOT2* and *FgNOT4*, were significantly altered but not of other Ccr4-Not subunits, suggesting that they function within the context of Not module. In addition, transcript levels of *FgNOT1* and *FgNOT4* was decreased, whereas *FgNOT2* transcript level was highly increased in the Δ*Fgnot3* compared to wild type with unknown reason. Because the feedback regulation often occurs in protein complexes (Yu et al. 2014), *Fg*Not2 might be a direct interactor of *Fg*Not3 but not of *Fg*Not1 and *Fg*Not4. The heterodimerization of the Not module in the ScNot1-ScNot2-ScNot5 or *C*Not1-*C*Not2-*C*Not3 forms a platform for macromolecular interactions (Bhaskar et al. 2013; Boland et al. 2013). While *Sc*Not3/5 and *Sc*Not2 seems to function together (Collart et al. 2013), and *Sc*Not3 directly interacts with *Sc*Not4 and *Sc*Not5 in yeast (Collart and Struhl 1994; Oberholzer and Collart 1998), there is no interaction between *C*Not3 and *C*Not4 in human (Albert et al. 2000). The interaction between these proteins in *F. graminearum* need to be confirmed, but these differences might be attributed to a different composition of the complex or the evolutionary divergence in yeast, filamentous fungi, and human.

We further functionally characterized the Not module of the

Ccr4-Not complex in *F. graminearum*. *FgNOT1* is an essential gene, as reported in other eukaryotes (Son et al. 2011b). Δ*Fgnot2* and Δ*Fgnot4* mutants had pleiotropic effects on phenotypes, including vegetative growth, sexual and asexual production, and virulence, similar to the impacts of Δ*Fgnot3*, suggesting that the Not module composed of *Fg*Not1-4 is also conserved in *F. graminearum*. In yeast, the association of all Ccr4-Not subunits is essential for cell viability, although it remains unclear whether each subunit functions only within the context of a complex or has distinct roles outside of the complex (Collart et al. 2013). For example, *Sc*Not4 mainly functions in regulation of proteasome integrity, whereas the *Sc*Not2-3/5 module has more fundamental roles. Therefore, Δ*Sc*Not2 or Δ*Sc*Not5 showed more pronounced growth defects than Δ*Sc*Not4 (Collart et al. 2013). Consistently, *FgNOT4* deletion had a slight effect on phenotypes, although deletion of *FgNOT2* resulted in mostly indistinguishable phenotypic defects compared to Δ*Fgnot3* mutants.

FgNOT2, *FgNOT3,* and *FgNOT4* are negative regulators of ZEA and/or trichothecenes production. Whereas Δ*Fgnot2* and Δ*Fgnot4* mutants produced significantly higher levels of ZEA and/or trichothecenes, Δ*Fgnot3* accumulated more than 40-fold higher levels of both ZEA and trichothecenes compared to wild type. The Not module of the Ccr4-Not complex appears to regulate upstream genes or

transcriptional regulatory elements participating in the diverse regulation of multiple secondary metabolite biosynthetic clusters. Moreover, highly accumulated mycotoxins might affect the physiologies of the Δ*Fgnot2*, Δ*Fgnot3*, and Δ*Fgnot4* mutants. Although direct biological functions of mycotoxins have not been reported in *F. graminearum*, overproduction of secondary metabolites often leads to unexpected developmental defects. All of the 13 transcription factor mutants overproducing ZEA and/or trichothecenes showed defective vegetative growth and/or reproduction (Son et al. 2011b), and *FgFlbA* deletion mutants accumulating both ZEA or trichothecenes at high levels also showed pleiotropic defects in *F. graminearum* (Park et al. 2012).

In summary, our study functionally characterized the Not3 subunit of the Ccr4-Not complex for the first time in filamentous fungi. *FgNOT3* is involved in hyphal morphogenesis and cellular differentiation, which are related to both sexual and asexual sporulation and virulence in *F. graminearum*. In addition, we found that the Not module of the Ccr4-Not complex of *F. graminearum* is conserved and involved in numerous characteristics, including vegetative growth, reproduction, virulence, and secondary metabolism.

Table S1. Primers used in this study.

Primer	Sequence (5'→3')	Description
Not3-5F	ATCCTCAAGACCTTGGCGGC	Forward and reverse primers for amplification of 5′-flanking region of *FgNOT3* with tail for the geneticin resistance gene cassette fusion
Not3-5R	gcacaggtacacttgtttagagGCGGTTGCTAAAGACAGACAGAG	
Not3-3F	ccttcaatatcatcttctgtcgTACGAACCCTTCGAGTGCCG	Forward and reverse primers for amplification of 3′-flanking region of *FgNOT3* with tail for the geneticin resistance gene cassette fusion
Not3-3R	GGCGGCTGACGAATGCTAAC	
Not3-5N	ACAAATGTACCTTTTCCCAAAGCTC	Forward and reverse nest primers for third fusion PCR for amplification of the *FgNOT3* deletion construct
Not3-3N	TGCGCCTCGGTGACTGATAG	
Gen-for	CGACAGAAGATGATATTGAAGG	Forward and reverse primers for amplification of the geneticin cassette from the pII99 vector
Gen-rev	CTCTAAACAAGTGTACCTGTG	
pBCATPH/comp 5′For	GTGAGCGGATAACAATTTCACACAG	Forward and reverse primers for amplification of hygromycin B resistance gene cassette from pBCATPH
pBCATPH/comp 3′Rev	GAGATCCTGAACACCATTTGTCTCA	

pIGPAPA/H2	TCGCTCCAGTCAATGACCGC	Forward nest primers for split marker amplification of hygromycin B resistance gene cassette
pU,pBC/H3	CGTTATGTTTATCGGCACTTTGC	Reverse nest primers for split marker amplification of hygromycin B resistance gene cassette
Gen-G2	GCAATATCACGGGTAGCCAACG	Forward nest primers for split marker amplification of geneticin resistance gene cassette
Gen-G3	GGGAAGGGACTGGCTGCTATTG	Reverse nest primers for split marker amplification of geneticin resistance gene cassette
pIGPAPA-sGFP	GTGAGCAAGGGCGAGGAGCTG	Forward and reverse primers for amplification of Gfp-*HYG* construct from pIGPAPA
Hyg-F1	GGCTTGGCTGGAGCTAGTGGAGG	
Not3-5F com	GAAAAGGGAGTCCAACAGGCAATAA	Forward primer for amplification of *FgNOT3* with tail for the hygromycin B resistancegene cassette fusion
Not3-5N com	GAAAAACCACGTCATTGAAACTATCCC	Forward nest for amplification of *FgNOT3* with tail for the hygromycin B resistancegene cassette fusion

Not3- 3N com	tgagacaaatggtgttcaggatctcGAGGCTGCAGCAAGAAAAAGAGGT	Reverse primer for amplification of *FgNOT3* with tail for the hygromycin B resistancegene cassette fusion
STUA-rt-F	CAGAACGGAAATGATGGTGGACTC	For realtime-PCR of *STUA*
STUA-rt-R	ATTGGAAAGAGGCTGGTGAAGGT	
HTF1-rt-F	GGAAGAAGAGCTGAGGTGGGACAT	For realtime-PCR of *HTF1*
HTF1-rt-R	TGGAAGTTGGGGGAGCGGT	
REN1-rt-F	ACGACAGACTTGAATCGCCTGACA	For realtime-PCR of *REN1*
REN1-rt-R	TATCGTGCCACATCGTATCCAGCA	
FLBC-rt-F	TTCAGCTCCAAGGTGTCTTCCAGT	For realtime-PCR of *FLBC*
FLBC-rt-R	ACAGAGAAATGTCGACCACAGCCT	
ABAA-rt-F	ACTCAGGAAGCTTTGACCACGGC	For realtime-PCR of *ABAA*
ABAA-rt-R	GGGCTCTGGTAGGGGTTGACAGTA	
WETA-rt-F	GTTCCAGGTACTCCCACTGCCAT	For realtime-PCR of *WETA*
WETA-rt-R	ACGTTCTCGTCGCGCTTTGGT	
CAF130-rt-F	TCATTAGACGTTCGACCCCATTTC	For realtime-PCR of *CAF130*
CAF130-rt-R	TCGGGTTGGTGATGTAGATGGTG	

CAF1-rt-F	TACTGAGTTTCCGGGTGTCGTTTC	For realtime-PCR of *CAF1*
CAF1-rt-R	AAACTGCCACGAACAAGGGAAAG	
NOT1-rt-F	TCAGCCAAACCTCCCAACAAGA	For realtime-PCR of *NOT1*
NOT1-rt-R	CAAGGAGGCATAGGCACTGACAA	
NOT4-rt-F	CCGTGCCAACATCCAGAAGAAC	For realtime-PCR of *NOT4*
NOT4-rt-R	CTCGGGCTTTCGCAGTGTCTT	
CAF40-rt-F	TCTACCCCTTTCTCAACACCACCTC	For realtime-PCR of *CAF40*
CAF40-rt-R	CCATTGTCGTCGAGCAGGATTT	
DHH1-rt-F	CGCCTTTGTCATCCCCACCT	For realtime-PCR of *DHH1*
DHH1-rt-R	ATTCGCTAAGGTCGGCAACATTC	
NOT2-rt-F	GTCCAACGCCAACCAGTCATCTAT	For realtime-PCR of *NOT2*
NOT2-rt-R	GAGGTTTGGTTGAGTGGTGGGA	
NOT3-rt-F	GATCCCAAAGAGCAGGCAAAGG	For realtime-PCR of *NOT3*
NOT3-rt-R	TGCCTTGATGCCACTTATGTCGT	
CCR4-rt-F	CACCCCTCTCAGACACAACACCA	For realtime-PCR of *CRR4*
CCR4-rt-R	GCATGCGCTCGTTCGGACT	

UBH-rt-F	GTTCTCGAGGCCAGCAAAAAGTCA	For realtime-PCR of *UBH*
UBH-rt-R	CGAATCGCCGTTAGGGGTGTCTG	
Not3-cloning-F	GCATGACCAGTGTGCTGGATGGCGGCAAGGAAACTGGCCC	Forward and reverse primer for amplification of cDNA of *FgNOT3*
Not3-cloning-R	GCATGATCTAGATAAAAAGATGGGGGAACATGTTTGATACTGC	
Not3-cloning seq-F	CGGACTACTAGCAGCTGTAATACGACTC	Forward and reverse primer for amplification of sequencing colonies containing plasmid construct pYES2-*FgNOT3*
Not3-cloning seq-R	GGTTGTCTAACTCCTTCCTTTTCGGT	
Not4-5F	GACCAGCAAAGAAGACACCGTAAAG	Forward and reverse primers for amplification of 5′-flanking region of *FgNOT4* with tail for the geneticin resistance gene cassette fusion
Not4-5R	gcacaggtacacttgtttagagTGTCGTGTGATTAGTTTGAAAGGTGGTA	
Not4-3F	ccttcaatatcatcttctgtcgTTCACGTAACGACAGGGCAGAGT	Forward and reverse primers for amplification of 3′-flanking region of *FgNOT4* with tail for the geneticin resistance gene cassette fusion
Not4-3R	CAGCGAACGACCAGACCACAGT	
Not4-5N	GCAGCGGTGTTGTCTATCAGGTTT	Forward and reverse nest primers for third fusion PCR for amplification of the *FgNOT4* deletion construct
Not4/3N	AAAAGCACAACCAAAACCCAAGAAC	

Not4-5F com	CCATCACCCAGGCACCGTATC	Forward primer for amplification of *FgNOT4* with tail for the hygromycin B resistancegene cassette fusion
Not4-5N com	GAGAATCTTAGCGGCAGAACAGTGG	Forward nest for amplification of *FgNOT4* with tail for the hygromycin B resistancegene cassette fusion
Not4-3N com	tgagacaaatggtgttcaggatctcCTCTAACATTGATGCTATCGCTTCGT	Reverse primer for amplification of *FgNOT4* with tail for the hygromycin B resistancegene cassette fusion
Not2-5F	AAGTAGAGGAGTGGTTGGAAGTTGGTAA	Forward and reverse primers for amplification of 5′-flanking region of *FgNOT2* with tail for the geneticin resistance gene cassette fusion
Not2-5R	gcacaggtacacttgtttagagCGCGAGCGACTAAGGTAAGGTG	
Not2-3F	ccttcaatatcatcttctgtcgTTAGGTGAGGGAGCATGGTGATTG	Forward and reverse primers for amplification of 3′-flanking region of *FgNOT2* with tail for the geneticin resistance gene cassette fusion
Not2-3R	CAGGGGCCGTTATTGTTGTTCAG	
Not2-5N	AACGGAACTCAACCAAGTCAAGGA	Forward and reverse nest primers for third fusion PCR for amplification of the *FgNOT2* deletion construct
Not2-3N	GCGATACGGCATCTAGCTTGTTCT	

Not2-5F com	CGACGCGAAAGAGGAGAGAAAT	Forward primer for amplification of *FgNOT2* with tail for the hygromycin B resistancegene cassette fusion
Not2-5N com	GTTGGACCTTTTCCCCGTGG	Forward nest for amplification of *FgNOT2* with tail for the hygromycin B resistancegene cassette fusion
Not2-3N com	tgagacaaatggtgttcaggatctcCGACAAGCCAGCCCTCAG TAAT	Reverse primer for amplification of *FgNOT2* with tail for the hygromycin B resistancegene cassette fusion

LITERATURE CITED

Albert TK, Lemaire M, van Berkum NL, Gentz R, Collart MA, Timmers HTM. 2000. Isolation and characterization of human orthologs of yeast CCR4–NOT complex subunits. *Nucleic Acids Res* **28**: 809-817.

Bai Y, Salvadore C, Chiang Y-C, Collart MA, Liu H-Y, Denis CL. 1999. The *CCR4* and *CAF1* proteins of the *CCR4-NOT* complex are physically and functionally separated from *NOT2*, *NOT4*, and *NOT5*. *Mol Cell Biol* **19**: 6642-6651.

Bhaskar V, Roudko V, Basquin J, Sharma K, Urlaub H, Séraphin B, Conti E. 2013. Structure and RNA-binding properties of the Not1–Not2–Not5 module of the yeast Ccr4–Not complex. *Nature Struct Biol* **20**: 1281-1288.

Boenisch MJ, Schäfer W. 2011. *Fusarium graminearum* forms mycotoxin producing infection structures on wheat. *BMC Plant Biol* **11**: 110.

Boland A, Chen Y, Raisch T, Jonas S, Kuzuoğlu-Öztürk D, Wohlbold L, Weichenrieder O, Izaurralde E. 2013. Structure and assembly of the *NOT* module of the human CCR4–NOT complex. *Nature Struct Biol* **20**: 1289-1297.

Bowden RL, Leslie JF. 1999. Sexual recombination in *Gibberella zeae*. *Phytopathology* **89**: 182-188.

Cappellini R, Peterson J. 1965. Macroconidium formation in submerged cultures by a non-sporulating strain of *Gibberella zeae*. *Mycologia*: 962-966.

Chen J, Rappsilber J, Chiang Y-C, Russell P, Mann M, Denis CL. 2001. Purification and characterization of the 1.0 MDa CCR4-NOT complex identifies two novel components of the complex. *J Mol Biol* **314**: 683-694.

Cheng S, Clancy CJ, Checkley MA, Zhang Z, Wozniak KL, Seshan KR, Jia HY, Fidel P, Cole G, Nguyen MH. 2005. The role of *Candida albicans NOT5* in virulence depends upon diverse host factors in vivo. *Infect Immun* **73**: 7190-7197.

Collart MA. 2003. Global control of gene expression in yeast by the Ccr4-Not complex. *Gene* **313**: 1-16.

Collart MA, Panasenko OO. 2012. The Ccr4–not complex. *Gene* **492**: 42-53.

Collart MA, Panasenko OO, Nikolaev SI. 2013. The Not3/5 subunit of the Ccr4-Not complex: a central regulator of gene expression that integrates signals between the cytoplasm and the nucleus in eukaryotic cells. *Cell Signal* **25**: 743-751.

Collart MA, Struhl K. 1994. *NOT1 (CDC39)*, *NOT2 (CDC36)*, *NOT3*, and *NOT4* encode a global-negative regulator of transcription that differentially affects TATA-element utilization. *Genes Dev* **8**: 525-537.

Collart MA, Timmers H. 2004. The eukaryotic Ccr4-Not complex: a regulatory platform integrating mRNA metabolism with cellular signaling pathways? *Prog Nucleic Acid Res Mol Biol* **77**: 289-322.

Denis CL. 1984. Identification of new genes involved in the regulation of yeast alcohol dehydrogenase II. *Genetics* **108**: 833-844.

Desjardins AE. 2006. *Fusarium mycotoxins: chemistry, genetics, and biology*. American Phytopathological Society Press, St Paul, MN, USA.

Draper MP, Salvadore C, Denis CL. 1995. Identification of a mouse protein whose homolog in *Saccharomyces cerevisiae* is a component of the CCR4 transcriptional regulatory complex. *Mol Cell Biol* **15**: 3487-3495.

Gietz RD, Schiestl RH. 2007. Frozen competent yeast cells that can be transformed with high efficiency using the LiAc/SS carrier DNA/PEG method. *Nat Protoc* **2**: 1-4.

Goldstrohm AC, Wickens M. 2008. Multifunctional deadenylase complexes diversify mRNA control. *Nature Rev Mol Cell Biol* **9**: 337-344.

Goswami RS, Kistler HC. 2004. Heading for disaster: *Fusarium graminearum* on cereal crops. *Mol Plant Pathol* **5**: 515-525.

Guenther JC, Trail F. 2005. The development and differentiation of *Gibberella zeae* (anamorph: *Fusarium graminearum*) during

colonization of wheat. *Mycologia* **97**: 229-237.

Han YK, Kim MD, Lee SH, Yun SH, Lee YW. 2007. A novel F-box protein involved in sexual development and pathogenesis in *Gibberella zeae*. *Mol Microbiol* **63**: 768-779.

Harris SD. 2005. Morphogenesis in germinating *Fusarium graminearum* macroconidia. *Mycologia* **97**: 880-887.

Hong S-Y, So J, Lee J, Min K, Son H, Park C, Yun S-H, Lee Y-W. 2010. Functional analyses of two syntaxin-like *SNARE* genes, *GzSYN1* and *GzSYN2*, in the ascomycete *Gibberella zeae*. *Fungal Genet Biol* **47**: 364-372.

Hu G, Kim J, Xu Q, Leng Y, Orkin SH, Elledge SJ. 2009. A genome-wide RNAi screen identifies a new transcriptional module required for self-renewal. *Genes Dev* **23**: 837-848.

Jansen C, Von Wettstein D, Schäfer W, Kogel K-H, Felk A, Maier FJ. 2005. Infection patterns in barley and wheat spikes inoculated with wild-type and trichodiene synthase gene disrupted *Fusarium graminearum*. *Proc Natl Acad Sci USA* **102**: 16892-16897.

Jiang J, Liu X, Yin Y, Ma Z. 2011. Involvement of a velvet protein *Fg*VeA in the regulation of asexual development, lipid and secondary metabolisms and virulence in *Fusarium graminearum*. *PLoS One* **6**: e28291.

Jin R, Dobry CJ, McCown PJ, Kumar A. 2008. Large-scale analysis of

yeast filamentous growth by systematic gene disruption and overexpression. *Mol Biol Cell* **19**: 284-296.

Jonkers W, Dong Y, Broz K, Kistler HC. 2012. The Wor1-like protein Fgp1 regulates pathogenicity, toxin synthesis and reproduction in the phytopathogenic fungus *Fusarium graminearum*. *PLoS Genet* **8**: e1002724.

Kapitzky L, Beltrao P, Berens TJ, Gassner N, Zhou C, Wüster A, Wu J, Babu MM, Elledge SJ, Toczyski D. 2010. Cross-species chemogenomic profiling reveals evolutionarily conserved drug mode of action. *Mol Syst Biol* **6**: 451.

Kim H, Smith JE, Ridenour JB, Woloshuk CP, Bluhm BH. 2011. *HXK1* regulates carbon catabolism, sporulation, fumonisin B1 production and pathogenesis in *Fusarium verticillioides*. *Microbiology* **157**: 2658-2669.

Kim H-K, Yun S-H. 2011. Evaluation of potential reference genes for quantitative RT-PCR analysis in *Fusarium graminearum* under different culture conditions. *Plant Pathology J* **27**: 301-309.

Leslie JF, Summerell BA, Bullock S. 2006. *The Fusarium laboratory manual*. Blackwee Pub, Ames, IA.

Livak KJ, Schmittgen TD. 2001. Analysis of relative gene expression data using real-time quantitative PCR and the $2^{-\Delta\Delta CT}$ method. *Methods* **25**: 402-408.

Lysoe E, Pasquali M, Breakspear A, Kistler HC. 2011. The

transcription factor *Fg*StuAp influences spore development, pathogenicity, and secondary metabolism in *Fusarium graminearum*. *Mol Plant Microbe Interact* **24**: 54-67.

Maillet L, Tu C, Hong YK, Shuster EO, Collart MA. 2000. The essential function of Not1 lies within the Ccr4-Not complex. *J Mol Biol* **303**: 131-143.

Miller JE, Reese JC. 2012. Ccr4-Not complex: the control freak of eukaryotic cells. *Crit Rev Biochem Mol Biol* **47**: 315-333.

Min K, Son H, Lee J, Choi GJ, Kim J-C, Lee Y-W. 2012. Peroxisome function is required for virulence and survival of *Fusarium graminearum*. *Mol Plant Microbe Interact* **25**: 1617-1627.

Morita M, Oike Y, Nagashima T, Kadomatsu T, Tabata M, Suzuki T, Nakamura T, Yoshida N, Okada M, Yamamoto T. 2011. Obesity resistance and increased hepatic expression of catabolism-related mRNAs in *Cnot3*$^{+/-}$ mice. *EMBO J* **30**: 4678-4691.

Neely GG, Kuba K, Cammarato A, Isobe K, Amann S, Zhang L, Murata M, Elmén L, Gupta V, Arora S. 2010. A global in vivo *Drosophila* RNAi screen identifies *NOT3* as a conserved regulator of heart function. *Cell* **141**: 142-153.

Oberholzer U, Collart M. 1998. Characterization of *NOT5* that encodes a new component of the Not protein complex. *Gene* **207**: 61-69.

Ohara T, Inoue I, Namiki F, Kunoh H, Tsuge T. 2004. *REN1* is required for development of microconidia and macroconidia, but not of

chlamydospores, in the plant pathogenic fungus *Fusarium oxysporum*. *Genetics* **166**: 113-124.

Panepinto JC, Heinz E, Traven A. 2013. The cellular roles of Ccr4-NOT in model and pathogenic fungi - implications for fungal virulence. *Front Genet* **4**: 302.

Park AR, Cho A-R, Seo J-A, Min K, Son H, Lee J, Choi GJ, Kim J-C, Lee Y-W. 2012. Functional analyses of regulators of G protein signaling in *Gibberella zeae*. *Fungal Genet Biol* **49**: 511-520.

Proctor RH, Hohn TM, McCormick SP. 1995. Reduced virulence of *Gibberella zeae* caused by disruption of a trichothecene toxin biosynthetic gene. *Mol Plant Microbe Interact* **8**: 593-601.

Sambrook J, Russell DW. 2001. *Molecular cloning: a laboratory manual*. Cold Spring Harbor Laboratory Press, Cold Spring Harbor, NY.

Seo J-A, Kim J-C, Lee D-H, Lee Y-W. 1996. Variation in 8-ketotrichothecenes and zearalenone production by *Fusarium graminearum* isolates from corn and barley in Korea. *Mycopathologia* **134**: 31-37.

Son H, Kim M-G, Min K, Lim JY, Choi GJ, Kim J-C, Chae S-K, Lee Y-W. 2014. WetA is required for conidiogenesis and conidium maturation in the ascomycete fungus *Fusarium graminearum*. *Eukaryot Cell* **13**: 87-98.

Son H, Kim M-G, Min K, Seo Y-S, Lim JY, Choi GJ, Kim J-C, Chae S-

K, Lee Y-W. 2013. AbaA regulates conidiogenesis in the ascomycete fungus *Fusarium graminearum*. *PloS One* **8**: e72915.

Son H, Lee J, Park AR, Lee Y-W. 2011a. ATP citrate lyase is required for normal sexual and asexual development in *Gibberella zeae*. *Fungal Genet Biol* **48**: 408-417.

Son H, Seo Y-S, Min K, Park AR, Lee J, Jin J-M, Lin Y, Cao P, Hong S-Y, Kim E-K. 2011b. A phenome-based functional analysis of transcription factors in the cereal head blight fungus, *Fusarium graminearum*. *PLoS Pathog* **7**: e1002310.

Sutton J. 1982. Epidemiology of wheat head blight and maize ear rot caused by *Fusarium graminearum*. *Can J Plant Pathol* **4**: 195-209.

Szklarczyk D, Franceschini A, Kuhn M, Simonovic M, Roth A, Minguez P, Doerks T, Stark M, Muller J, Bork P. 2011. The STRING database in 2011: functional interaction networks of proteins, globally integrated and scored. *Nucleic Acids Res* **39**: D561-D568.

Venturini G, Rose AM, Shah AZ, Bhattacharya SS, Rivolta C. 2012. *CNOT3* is a modifier of *PRPF31* mutations in retinitis pigmentosa with incomplete penetrance. *PLoS Genet* **8**: e1003040.

Villanyi Z, Ribaud V, Kassem S, Panasenko OO, Pahi Z, Gupta I,

Steinmetz L, Boros I, Collart MA. 2014. The Not5 subunit of the Ccr4-Not complex connects transcription and translation. *PLoS Genet* **10**: e1004569.

Yu J-H, Hamari Z, Han K-H, Seo J-A, Reyes-Domínguez Y, Scazzocchio C. 2004. Double-joint PCR: a PCR-based molecular tool for gene manipulations in filamentous fungi. *Fungal Genet Biol* **41**: 973-981.

Yu J, Son H, Park AR, Lee S-H, Choi GJ, Kim J-C, Lee Y-W. 2014. Functional characterization of sucrose non-fermenting 1 protein kinase complex genes in the Ascomycete *Fusarium graminearum*. *Curr Genet* **60**: 35-47.

Zheng W, Zhao X, Xie Q, Huang Q, Zhang C, Zhai H, Xu L, Lu G, Shim W-B, Wang Z. 2012. A conserved homeobox transcription factor Htf1 is required for phialide development and conidiogenesis in *Fusarium* species. *PloS One* **7**: e45432.

ABSTRACT IN KOREAN

Fusarium graminearum 의 열충격반응 관련 유전자 기능연구

Duc Cuong Bui

초록

*Fusarium graminearum*은 주요 곡류에 이삭마름병을 일으키며 곰팡이 독소를 생성하여 인축에 중독증을 일으키는 중요한 병원균이다. 많은 연구자들은 *F. graminearum*에 의한 병 제어를 목표로 곰팡이 생활사, 이차대사산물생성, 기주와의 상호작용 등에 대한 다양한 분자유전학적 연구들을 진행하고 있다. 이 연구에서는 우선 열충격반응에 대한 게놈수준에서의 이해를 위해 전사체 분석을 수행하여 *F. graminearum*의 열충격반응을 분자수준에서 이해코자 하였다. Heat shock protein 90 (*Fg*Hsp90)는 *F. graminearum*에서 필수적인 유전자로 유도성 프로모터를 활용하여 기능연구를 수행하였다. *Fg*Hsp90는 열 스트레스에 반응하여 핵 내로 이동하며 열충격반응에서 핵심적인 역할을 하였다. 뿐만 아니라 *Fg*Hsp90는 *F. graminearum*의 균사생장, 유·무성

생식, 병원성에도 중요한 역할을 함을 세부 기능연구를 통해 밝혔다. 다음으로 Ccr4-Not 복합체의 서브유닛들에 대한 기능연구를 수행하였다. *Fg*Not3 서브유닛은 곰팡이의 형태발생과, 유·무성 생식, 병원성에 중요한 역할을 하며 특히 곰팡이독소 생성(trichothecenes and zearalenone)과정에서는 네거티브 레귤레이터로서 작용함을 알 수 있었다. Ccr4-Not 복합체의 다른 서브유닛인 *FgNOT2*과 *FgNOT4*에 대한 추가 연구를 통해 이들 서브유닛들은 Ccr4-Not 복합체로서 주로 작용을 하지만 각 서브유닛별 특화된 기능도 갖고 있음을 예상할 수 있었다. 이 연구에서는 병원성곰팡이에서 최초로 Hsp90과 Ccr4-Not 복합체의 기능을 분자유전학적 수준에서 알아보고자 하였으며 곰팡이에서의 열충격 반응 메커니즘과 발달과정을 이해하기 위한 중요한 단초를 제공하였다.

주요어: *Fusarium graminearum*, 이삭마름병, heat shock protein 90, Ccr4-Not complex, 곰팡이 발달, 분생포자, 병원성

학번: 2013-30788